LATERAL DEFLECTION OF A WEB DUE

TO A DIFFERENTIALLY

LOADED NIP

By

MOHAMMAD NOMAN AHMAD

Bachelor of Science

Oklahoma State University
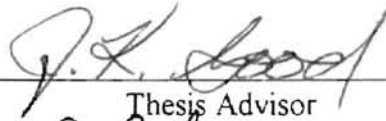
Stillwater, Oklahoma
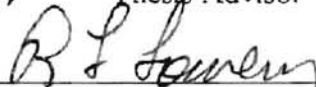
1995

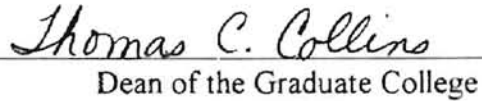# LATERAL DEFLECTION OF A WEB DUE

TO A DIFFERENTIALLY

LOADED NIP

Thesis Approved:

_____
Thesis Advisor

_____

_____

_____
Dean of the Graduate College

ii

ACKNOWLEDGMENTS

I would like to thank Dr. J. Keith Good for his guidance and advise throughout the development of this investigation. Without his help and supervision, I would not have completed this work. I am truly grateful to have him as my advisor in my graduate studies. No amount of gratitude can show my appreciation for him. This has been one of the most rewarding educational experiences I have ever had.

I am also grateful to my committee members, Dr. John J. Shelton and Dr Richard Lowery, for their constructive advise and expertise to help improve this thesis. I am thankful to Dr. Shelton for the models used in this investigation and his expert advise during the development of the study. I appreciate Dr. Lowery for the use of his durometer tester and his advise.

I appreciate the opportunity presented by Dr. C.E. Price to help teach the Materials Science Labs. This job allowed me to help other students developing as engineers. This was a very rewarding experience for myself.

Special thanks are due for the people I worked with at the research center. Ron Markum, Robert Taylor, Rod Brakhage, Robert Steves, Hung Nguyen, and Jeff Henning helped and supported this research directly or indirectly.

Finally, I would like to express my extreme gratitude to my parents, Moin and Quresha Ahmad. Their love and patience made this possible.

TABLE OF CONTENTS

LIST OF TABLES

LIST OF FIGURES

NOMENCLATURE

a	Half contact width of rubber covered rolls
A	Durometer
δ	Radial deflection of rubber covered rolls
D	Roll Diameter
E	Young's Modulus or modulus of elasticity
E_a	Modulus of elasticity as a function half contact width
E_c	Compressive modulus of rubber
ε	Strain at the edge of the web
$\Delta\varepsilon$	Change in strain from one edge of the web to the other
F	Force or load
F/W	Effective nip load
k	Factor used by Lindley in equation (1)
K	Stiffness
K_s	Specific stiffness
L	Length of the web prior to the nip
M	Moment
M_L	Moment at the length of the web
NLL	Load applied on left side of nip

NLR	Load applied on right side of nip
NRW	Nip roll width
QLeft	Effective load at left edge of nip
QRight	Effective load at right edge of nip
QLW	Effective load at left edge of web
QRW	Effective load at right edge of web
R_o	Undeflected rubber covered roll radius
S	Shape factor
t	Rubber cover thickness
T	Web tension
$\Delta V/V$	Change in velocity per velocity or strain
θ	Angle of rotation of roller or web
W	Nip width
WW	Distance from load applied on nip to edge of nip rollers
x	Location along the length of the web prior to the nip
Y	Lateral deflection of web

Chapter I

Introduction

A web is a thin continuous material. Examples include paper, plastic film, cloth, and aluminum foil. Web materials are flexible and cannot support bending alone. A web is usually stored in the form of a roll.

Web handling involves the transportation and processing of the material. Web handling includes slitting, splicing, coating and winding. Transportation usually involves long bands of web running along with the aid of rolls. Web handling improves processes by eliminating defects and losses. New techniques are created by these improvements.

Any type of web handling work involves the use of rolls. These rolls are either free spinning or driven. Rolls include the cores used to wind the material for storage to the rolls used for the transportation of the web The rolls can be metal, paper, wood, plastic, or rubber covered. A nip is any two rolls in contact as shown in figure 1-1. A common example is a nip roll used during the winding process. Winding is the procedure used to form the web into a roll. The core is the hollow tube used as the base for the rolls. Surface winding uses the nip roll to control the tension of the web being wound. The nip also controls the air entrained in the wound roll. Rolls are important in web handling.

During the processing of the web, the material travels along with the aid of rolls. Edge detectors sense the edge of the web by optical or pneumatic means and adjustments are made if the web edge strays laterally from the point of guidance. The adjustments
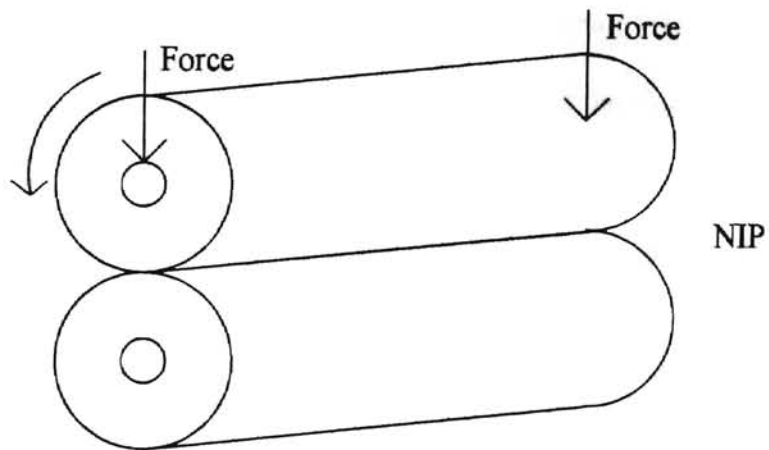
Figure 1-1: Illustration of a Nip

could be made by misaligning a roller on the entering side of the edge sensor as shown in figure 1-2. This technique is a popular form for lateral web guidance.
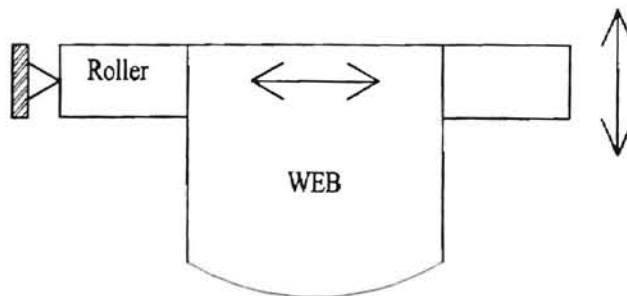
Figure 1-2: Movement of an end pivoted roller to adjust the lateral position of the web

Lateral movement of web has caused problems also. Too much movement can cause slackness to occur in the web. Slackness in a web is defined as when the web loses tension across some portion of the width.. When this happens the slack web may go through a nip or wound on to a roll causing creases or wrinkles to form. Thus, too much lateral movement becomes a problem as far as waste of material and process time.

This research focuses on rubber covered nip rollers. Non-uniform nip loading has been proven to be a means of laterally moving a web. Rubber is a nearly incompressible substance and when loaded in the geometry of the nip the rubber velocity increases as it passes through the contact zone. This is analogous to a problem in which a fluid is

passing through a reduced cross-section channel which perhaps expands back to a cross-section of the original dimensions. If the mass flow rate of the incompressible substance is assumed to be constant, then the velocity of the substance must increase as it passes through the constriction. It also follows that as the constricted cross-section becomes smaller that the velocity must increase even higher. Thus a set of rubber covered nip rollers with non-uniform nip loading will have a variation in velocity across their width in the contact zone.

A web being transported which encounters a set of such rollers will attempt to achieve the velocity of the rubber coverings in the contact zone. Thus in conditions in which the nip loading is non-uniform it should be expected that the web will have non-uniform velocity across its width. A variation in velocity across the width of a web is indicative of a variation in strain and therefore stress across the width. When integrated this stress will result in a moment which will be shown to produce the lateral deformation of the web.

The objective of this research will be to quantify and experimentally verify the lateral deformations of a web due to non-uniform nip loading with rubber covered rollers.

Chapter II

Literature Survey

A literature study in the area of web steering due to uneven nip loading was performed. Little work has been done in this area. Some research has been done in the area of rubber covered rolls for load and compression relationships. The following resources were used to develop or help in the algorithms used to predict the steering effect of a differentially loaded nip.

Lindley [8] presented a load-deformation relationship. Using approximate relationships derived for load compression of rubber blocks at low strains, Lindley expanded the relationships to rubber-covered rollers at larger deformations, equation (1). This was done by considering Young's modulus to be independent of the strain in the material.

$$\frac{F}{W} = E\sqrt{tD}\left[\alpha_R + \frac{kD}{t}\beta_R\right] \qquad (1)$$

$$\alpha_R = \frac{8}{3}\ln\left[\frac{1+\sqrt{u}}{1-\sqrt{u}}\right] - \frac{16}{3}\sqrt{u}, \; \beta_R = \ln\left[\frac{1+\sqrt{u}}{1-\sqrt{u}}\right] - \frac{10\sqrt{u}}{3(1-u)} + \frac{4\sqrt{u}}{3(1-u)^2} \; \text{and} \; u = \frac{\delta}{t}$$

$$E_c = \frac{4}{3}E(1+kS^2) \qquad (2)$$

$$S = \frac{\sqrt{D\delta}}{(t-\delta)}$$
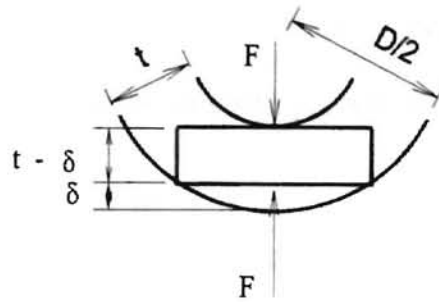
Figure 2-1: Illustration for Lindley's variables

Equation (1), however, requires a factor, k, to be determined empirically from equation (2). Equation (2) calculates compression modulus from shape factor and Young's modulus. Figure 2-1 illustrates the variables for Lindley's equations.

In 1964, Foreman [4] showed a relationship between rubber compression and the velocity of the strip passing through the pinch rolls. Foreman stated that the increased velocity is due to the increased length of contact between the compressed rubber and the strip passing through. Initially, Foreman used two sets of rubber covered rolls. One was 11 in. in diameter with a ¾ in. covering and the other was 30 in. in diameter with a 1 in. covering. The hardness of the covering ranged from 60 to 70 durometer. The strip was passed through and the top roll is loaded. By using a hand lever the bottom roll was turned by a single revolution. Figure 2-2 illustrates Foreman's experimental setup. After the full revolution was completed the length of movement is measured. The length of movement of the strip without any load was calculated from the diameter of a single roll. The difference divided by the initial length gave the percent increase. A steady increase was found due to added load. Increases up to 2 percent were found. Foreman also conducted experiments using one rubber covered roll and a steel roll. By doing so, the effects of different durometer and thickness on the increased movement were also shown. He also showed relationships between the compression of the rubber and the sheet

movement for different durometer and cover thickness. Foreman performed many experiments and developed many plots but didn't produce algorithms explaining the trends in the plots.
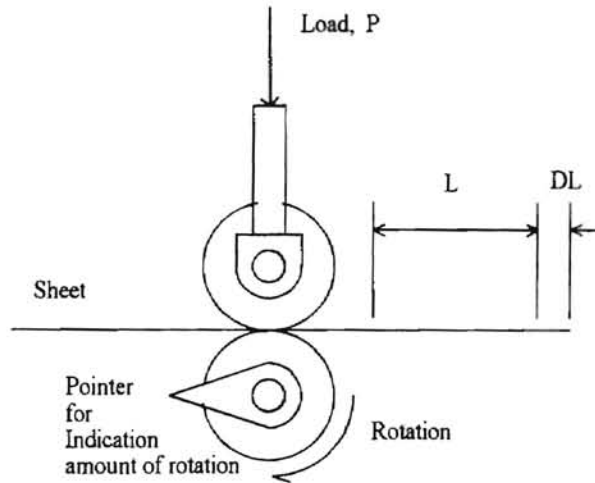
Figure2-2: Foreman's Experimental Setup

In 1994, Shelton [11] presented an informal report to Fife Corporation that outlines web steering due to differential nip loading across the width of the web. Shelton presented a relationship for calculating the effective nip load due to the radial deformation of the rubber, similar to Lindley's expression (1), and an algorithm to calculate the lateral movement of the web. These models were the primary basis for this investigation.

The following assumptions were applied in developing the equations for the effective nip load and lateral deflection:

Assumptions Regarding Nip Load versus Radial Deformation

1. The covering material behavior is that of natural rubber. When confined in the form of roll covering, it will be assumed that the covering is relatively incompressible.

2. Rubber covered nip rolls are identical in size and durometer. Therefore, symmetry will exist in the deformation of the rolls in contact

6

3. Small deflections of the rubber covered rolls occur when loaded. A relationship between contact width and radial deflection can be formulated.

Assumptions Regarding Lateral Deformation of the Rubber Covered Rolls

1. The entering web span prior to the nip is extremely long. Thus shear deformations are assumed to be negligible.

2. The lateral deformations are confined to the web span prior to the nip and results in a constant lateral offset in the downstream span.

Formulation of Effective Nip Load

Shelton starts with equation (3) using the definition for the stiffness of the rubber. The stiffness is defined [8] by the following equation:

$$K = \frac{AE}{t}$$

The stiffness is defined by the area of contact, A, multiplied by the modulus of elasticity, E, divided by the thickness, t. The area of contact for the case of two rubber covered rolls in contact would be 2Wa, where 2a represents the contact width and W is the width of the nip.

$$\frac{dF}{d\delta} = \frac{2WaE_a}{t} \qquad (3)$$

E_a is the modulus of elasticity that varies with the half contact width, a. Shelton developed the following equation for modulus by curve fit of data from a figure that relates compressive modulus to shape factor, S, and Shore A Durometer [4].

$$E_a = 31e^{0.048A}\left[1 + 1.7S^{(2.0-0.004A)}\right] \qquad (4)$$

Shape factor is defined as the loaded area per force free area [3]. By definition, shape factor becomes the following equation for a loaded rubber covered roll.

$$ShapeFactor = \frac{2aW}{2t(2a+W)}$$

For small values of half contact width compared to nip width, the shape factor becomes a/t. By applying the Pythagorean Theorem to figure 2-3, the following equation is formulated:

$$R_o^2 = a^2 + (R_o - \delta)^2$$

For small values of δ, the following equation relates the radial deflection, δ, to half contact width, a:

$$a = \sqrt{2R_0\delta} \qquad (5)$$
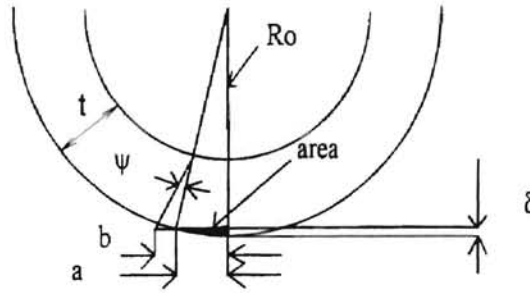
Figure 2-3: Side view of Rubber covered roll radial deflection

Combining and rearranging equations (3), (4), and (5) yields the following equation:

$$\frac{dF}{W} = \left[31e^{0.048A}\left(\frac{2R_0}{t}\right)^{1/2}\left(\frac{\delta}{t}\right)^{1/2} + 105.4e^{0.048A}\left(\frac{2R_0}{t}\right)^{(1.5-0.002A)}\left(\frac{\delta}{t}\right)^{(1.5-0.002A)} \right] t\frac{d\delta}{t} \qquad (6)$$

Integrating equation (6) by using δ/t as the independent variable yields the following equation:

$$\frac{F}{W} = t\left[41.3e^{0.048A}\sqrt{\frac{2R_0}{t}}\left(\frac{\delta}{t}\right)^{3/2} + \frac{105.4e^{0.048A}}{2.5-.002A}\left(\frac{2R_0}{t}\right)^{(1.5-.002A)}\left(\frac{\delta}{t}\right)^{(2.5-.002A)} \right] \qquad (7)$$

8

Components of equation (7) include the radius of the roll, the thickness of the covering, the durometer, and the radial deformation of the rubber.

Formulation of Lateral Deflection

The following 2nd order differential equation for an entering span was developed by Shelton in his thesis [12]:

$$\frac{d^2y}{dx^2} = -\frac{12M}{K_s W^3} \qquad (8)$$

The boundary equations that apply to the web entering the nip are as follows:
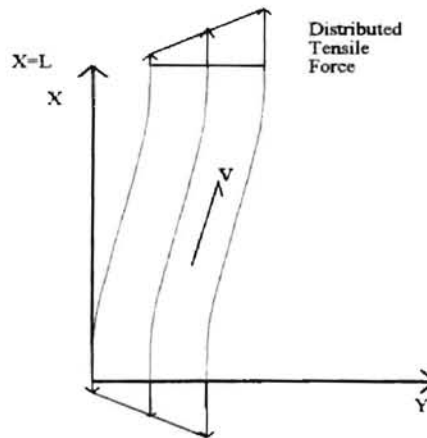
Figure 2-4: Illustration of "S" shape when web is deflected in the nip

1. $Y_0' = 0$
2. $Y_0 = 0$
3. $M_0 = -M_L$ (M_L Positive)
4. $Y_L' = 0$

From figure 2-4 and boundary condition (3), the moment can be calculated at any point along the web span using equation (9).

$$M = -M_L + \frac{2M_L + Ty_L}{L}x - Ty \qquad (9)$$

Equation (10) is used as a simplification.

$$K = \frac{\sqrt{\dfrac{12T}{K_s W}}}{W} \qquad (10)$$

By substituting equation (9) and equation (10), equation (8) becomes the following equation:

$$\frac{d^2 y}{dx^2} - K^2 y = K^2 M_L / T - K^2 (2M_L / T + y_L)\frac{x}{L} \qquad (11)$$

After integrating equation (11) twice and applying the boundary conditions, the following solution was derived.

$$Y = \frac{M_L}{T}\left[(\cosh Kx - 1) - \frac{\sinh KL}{\cosh KL - 1}(\sinh Kx - Kx)\right] \qquad (12)$$

It is easier to use the differential strain across the web width for the input to the previous equation rather than the moment. A distributed effective tension, T/W, is equated to an average effective tension plus the differential effective tension.. This is used to relate the moment to the differential tension in the web.

$$M_L = \frac{W}{12}\Delta T \qquad (13)$$

The following equation is the definition of specific stiffness:

$$K_s = \frac{\Delta T / W}{\Delta \varepsilon} \qquad (14)$$

By combining equation (13) and equation (14) and rearranging yields the following equation:

$$\frac{M_L}{T} = \frac{K_s W^2}{12T}\Delta \varepsilon \qquad (15)$$

Using equation (10) yields the following equation.

10

$$\frac{M_t}{T} = \frac{\Delta\varepsilon}{K^2 W} \qquad (16)$$

Substituting into equation (12) yields the equation for lateral deflection.

$$Y = \frac{\Delta\varepsilon}{K^2 W}\left[(\cosh Kx - 1) - \frac{\sinh KL}{\cosh KL - 1}(\sinh Kx - Kx)\right] \qquad (17)$$

The variable, $\Delta\varepsilon$, in this equation can be defined as the difference in travel per unit length of the two edges of the web. The strain is also the function of the difference in velocity per unit velocity of the edges. To determine the strain a study in nip behavior is required. The next equation is determined from the triangle area, shown in figure 2-3, equaling the half area displaced by the action of the nip:

$$\psi = \frac{4}{3}\frac{\delta a}{t^2} \qquad (18)$$

By assuming that the velocity ratio is proportional to the angle ψ and adding a proportional constant, the following equation for change in velocity per unit velocity. The constant was determined through a best fit of Foreman's data.

$$\frac{\Delta V}{V} = 0.25\frac{\delta a}{t^2} \qquad (19)$$

Substituting the equation for small deflections, the next equation relates the percentage velocity change to the roll radius, radial deflection of the roll and the rubber thickness.

$$\frac{\Delta V}{V} = \varepsilon = 0.35\frac{R_0^{1/2}\delta^{3/2}}{t^2} \qquad (20)$$

This equation gives the increment in strain, ε, in the web due to the speed increase of the rubber covering in the contact zone.

This investigation will attempt to verify the equation for the effective nip load, equation (7), and the lateral deflection equation, equation (17). Equation (7) assumes

small radial deflections, therefore, its usefulness applies to deflection in the rubber of this criteria. The formulation of the lateral deflection equation assumes that no web slackness exists. Another criteria for equation (17) is for the web span entering the nip should be sufficiently long.

Good [6] presented material at the October 1996 Web Handling Research Center IAB meeting that relates the incursion of web slackness due to a misaligned roller in a web line. Good was able to develop a relationship to find the critical angle of rotation of the roller at which slackness occurs.

$$\theta_{\sigma} = \frac{TL}{W^2 tE} \qquad (21)$$

Equation (21) determines the critical rotation angle of the back roll for a web span between a front and back roll. At this critical angle, slackness occurs in the web. For this situation, full contact and tension is maintained in the back roll when rotated. At the stationary front roll, the web maintains tension in only part of the contact. The situation with this investigation, observing figure 2-4, the loss of tension across the web, or slackness, occurs at two points at the nip and the leading roll. Equation (21) is effective since center of the entering span behaves like the rotating roll. Therefore, equation (21) can be applied to half the length of the entering span prior to the nip.

Little literature exists for the area of web due to uneven nip loading. Research, however, does exist for rubber covered rolls. Load and compression relationships have been researched. Lindley, for example, developed a relationship, equation (1), for calculating the effective nip load due to radial deflection. This equation was also experimentally verified by Lindley. Equation (1), however, requires a "k" factor to be

12

determined empirically from equation (2). Shelton also developed an equation for calculating effective nip load, equation (7). This equation is a function of radial deflection, rubber cover thickness, initial roll radius, and durometer. This equation has not been experimentally verified, however. Shelton also developed equation (17) to predict the lateral movement of the web due to uneven nip loading. The equation is related by the stiffness of the web, the nip width, entering span length, and the difference in strain from one edge to the other. The strain can be determined from equation (20). This equation is a function of radial deflection, roll radius, and rubber thickness. Once equation (7) has been verified, a source for determining radial deflection from effective nip load or vice versa can be established. This can then be used to determine the strain at the edges of the web from equation (20). Equation (17) can then be used to predict the lateral web deflection. The lateral deflection equation assumes that no web slackness exists. Using the equation developed by Good, equation (21), determines the critical angle of rotation when slackness occurs in the web. This equation is applied for a misaligned roller in a web line. For this situation the slackness occurs at the aligned roller. A deflected web due to non-uniform nip load forms an "S" shape. The slackness occurs at two points in this formation. One point is at the nip and the other is at the front roller. Equation (21), however, can be applied for a half of the length of the web entering the nip. This can then give an upper limit of useful lateral web deflection data. This study will attempt to verify equations (7) and (17) through experimental data.

Chapter III

Experimental Setup

A nip setup with loads that can be unevenly applied was needed to perform experiments. The setup required two rubber covered rolls of the same durometer. The setup needed to be installed on a web line that would allow continuous transport without changing the web during the experimental process. The setup had to be able to apply loads on both sides of the nip independently. An edge guiding mechanism needed to be used at the entry side to hold constant position for the web.

The Shelton machine at the Web Handling Research Center allows for continuous transport of a single strip of web. The web is spliced and taped together after being looped through the machine. The adjustable tension control roll adjusts the web line tension. Two identical springs supply force to either side of the tension roll. A DC motor drives a rubber covered roll that winds the web. The motor is controlled by the voltage supplied to it. A platform sits on top that can be adjusted horizontally. The nip setup was mounted to this table to be used with the test bed.

The first nip setup, illustrated in figure 3-1, was designed and built previously by Shelton for his Ph.D. study [12]. The original setup used Bellofram Super Cylinders to apply the load on the sides of the nip as illustrated. The mounts for these cylinders were pinned to the frame of the apparatus. The rolls were rubber covered of unknown

hardness. The rolls had to be modified to be free rolling in order to be used for the type of work expected. The top roll was modified so that bearings were pressed into the sides which made it turn upon the shaft. Bearing pillow blocks were used for the bottom shaft to turn freely. Since there wasn't enough room the pillow blocks had to be clamped to the frame.

Pressure Guages and Regulators

Bellofram
Super Cylinders

Cylinder Cup
Pinned and Clamped
to Frame

Rubber Covered Rolls

Linear
Guides
for
Roll
Shaft

Pillow Block
Bearing
Clamped to
Frame
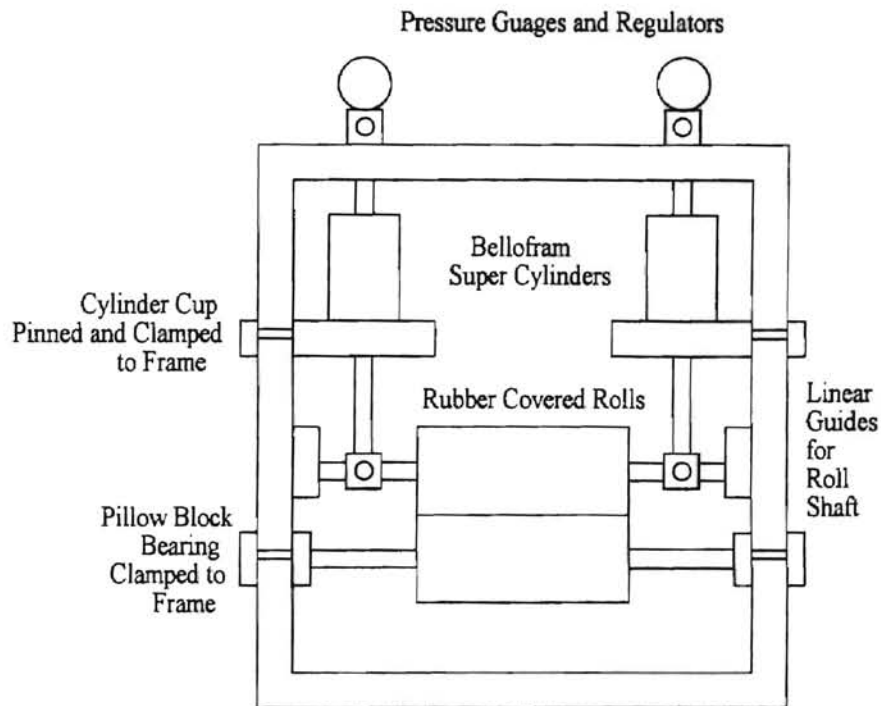
Figure 3-1: Illustration of original setup

This setup helped to determine that it was feasible to steer the web by unevenly loading the nip. Several tests were made in attempting to steer the web. The first tests were done by using one rubber covered roll and one metal roll. Paper, plastic and aluminum webs were used. The Fife guide at the front roll was turned off so that the steering of the web would be additive and, thus, run the web off the side of the nip. This formation demonstrated no web steering upon loading for each of the web used. Tests were also done by making an "S" shaped wrap around the rolls. The wrap formation is commonly used in industrial applications of nips. This technique emitted a high piercing

sound when the nip was loading while the web was running. This was thought to have been due to slippage occurring between the web and the nip rolls in compression. Lateral movement of the web was not seen in this formation either. The metal roll was taken out and replaced with another rubber covered roll. The paper web would tear when it passed through the loaded nip. The aluminum web didn't show any lateral displacement. The aluminum has high stiffness and was thought to steer better. No lateral displacement was seen. The plastic web showed movement. The only formation that showed lateral deflection was the two rubber covered rolls with plastic web running through the center of the nip. More lateral deflection was seen when less thick webs were used. Therefore, it was seen that an unevenly loaded nip with two rubber covered rolls could be used to laterally deflect plastic web.

The setup had limitations that would be needed for further work. The setup didn't allow independent control of the two sides being loaded. When an uneven load was applied, the top roll shaft would bind in the linear guides. The alignment of the two rolls needed to be of high accuracy. Misalignment has shown lateral displacement of web. The loading of the rolls also needed to be accurate. Pre-existing unevenness would skew data. The cylinder cups were pinned and clamped. More space was also desired so that other items can be mounted near the nip. A new design for the experimental setup was needed.

Towards a new experimental setup, three sets of rolls were designed and manufactured to be recovered with rubber of different durometer. These rolls were made with a core outside diameter of three inches. They were designed to be covered by rubber half inch in thickness and known hardness. Three different hardness values of 40, 55, and

70 durometer were to be used. These were chosen so that they would provide a broad range of durometer. The durometer of rubber is a measure of its hardness. The scales usually associated with the durometer are the International Rubber Hardness (IRHD) scale or the Shore A Durometer scale. These two scales are about the same. The rolls were sent to Mid-South Roller to be covered. Nitrile rubber was chosen because of its durability. After receiving the rolls, a Shore A Durometer tester was used to verify the hardness of the rubber. The tests determined that the actual durometer was 52, 60, and 78 instead of 40, 55, and 70 respectively. This made a difference considering the equations for lateral deflection are functions of the durometer. These rolls would be used in the new experimental setup.

The new experimental setup was designed and built. The new setup used the original Bellofram Super Cylinders. These cylinders have less frictional losses within the cylinder than most pneumatic cylinders. The pressure applied by the cylinder is closer to the pressure dialed on the gauges. The setup allowed total independent control of the two sides of the nip. The alignment between the rolls was accurate. Precision bearings were used to allow proper alignment of the rolls and cylinders as illustrated in figure 3-2 The new design also allowed flexibility in modifications. The new design was better suited for this study than the original setup.

The new nip setup was installed on the continuous loop web transport machine. The placement of the test apparatus was chosen so that the web running on the winder would pass through the center of the nip. A Fife Guide was used at the front roll in the entering span. This ensured that the web's position would be held constant on the front roll. Therefore the web would make an "S" shape as the web is steered in the nip. This

17
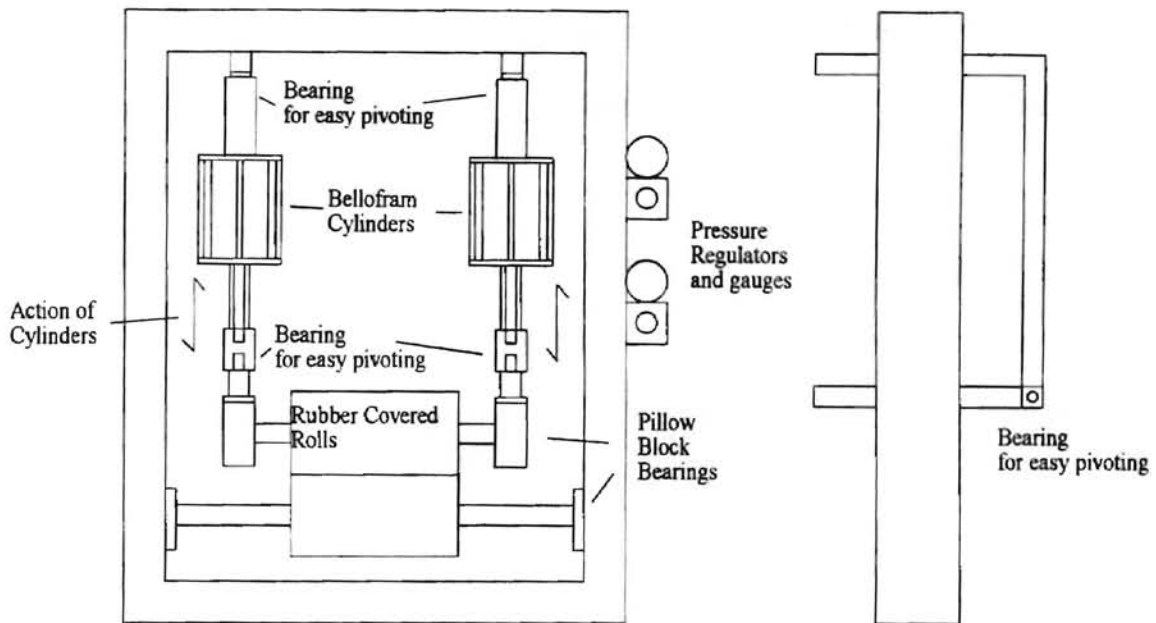
Figure 3-2: Illustration of new experimental setup

could clearly be seen when observed from the front roll looking down the edge of the web.

This was also the first indication of web steering through observation.
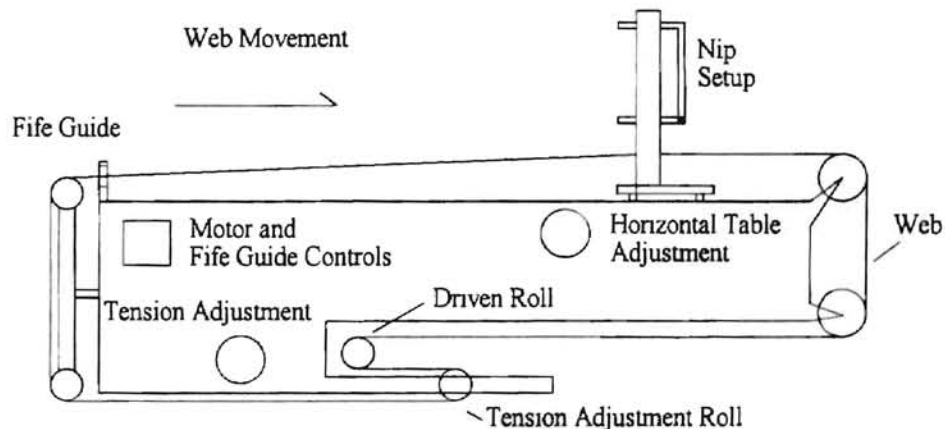
Figure 3-3: Illustration of new setup on continuous loop

The equations for the effective nip load and strain do not rely upon the properties

of the web. These equations require the durometer and characteristics of the rubber

covered rolls and the radial deformations. Only the lateral deflection equation relies upon

the stiffness and the entering length of the web. Polyester web was chosen to be used for

experimentation because of the availability at the lab. This material can be used

continuously without excessive damage. Also, it does not stretch as easily as other plastic web. The elastic modulus is 600,000 psi. The thickness is .002 in. and 6 in. wide. The dimensions and properties are used in the lateral deflection equation.

Although no set criteria for a long entering span was made, the experimental apparatus which was mounted on a movable plate was moved to the furthest part of the continuous loop from the first roll. It was placed to give the maximum entering length while still having room to work behind the nip. The length from the center of the front roll to the center of the nip was 71.25 inches.

A new experimental setup was designed and built. The new setup was designed specifically for this study. It was also designed so that modifications could be made easily if need be. Three sets of rubber covered rolls were made. They were chosen so that they would cover a wide range of durometer. Polyester web was chosen to be used for the forth coming experiments because of its availability. The length of the span of the web prior to the nip was set at the longest point on the experimental setup while having room for other devices to be installed. After the experimental setup was established, tests for the verification of equation (7) and (17) could begin.

Chapter IV

Experiment F/W and δ

Shelton [11] developed an equation relating the effective nip load to the radial deflection in the rubber rolls and the durometer of the rubber, equation (7). The independent variable in this equation for each set of rolls is the radial deflection. Rearranging equation (5), the following equation relates the radial deflection to the half contact width of the two rolls in contact.

$$\delta = \frac{a^2}{2R_0} \qquad (5a)$$

In order to obtain the half contact width, a Tek-scan sensor was used. The sensor is an array of force sensitive resistance sensors that provide a display of the pressure being applied to it. A sensor specifically designed to be used in a nip was used. The sensor requires two point calibration. The first point is usually near the smallest force used, while the second is the near the top of the range of use.

The sensor placed in the nip and loaded displays the pressure profile across the nip. The Tekscan software displays the profile on the computer monitor. The pixels on the display correspond to the resistor points on the sensor. The specifications of the sensor used is given in figure 4-1. Using the row width and the number of rows of sensor cells in the sensor, the length per cell was calculated. The pixels on the display were squares of .125 inches. By measuring the length of the pixels on the screen, the number of activated

cells were determined. Using the number of cells activated and the length per cell, the contact width was calculated. Half of this width is used in the equation above for calculating the radial deflection. The half width was determined for each set of rolls. The cylinders were loaded incrementally. Each cylinder was pressurized with equal pressure. The pressure applied was incremented by 3 psi to a maximum of 30 psi.
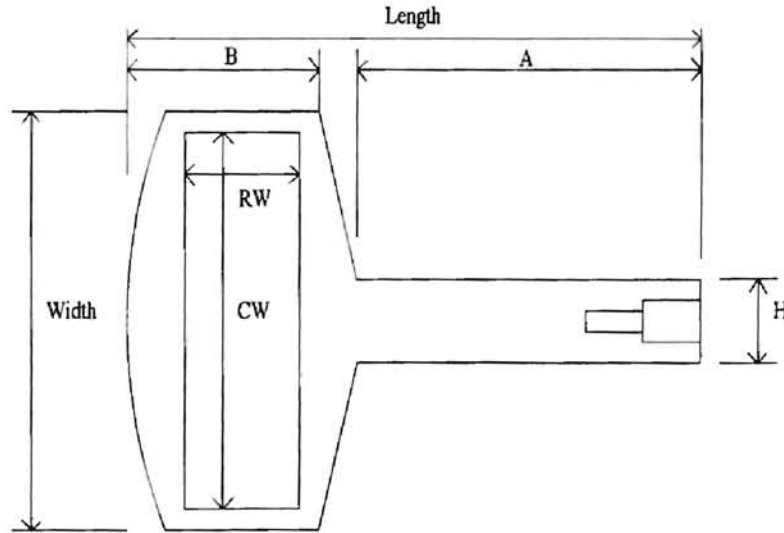
Figure 4-1: Illustration of Tek-scan sensor

Dimensions:

Length:	12.25 in.
width:	13.25 in.
Row x Col	34 x 44
Col width	11.75 in.
Col space	0.275 in.
Row width	0.825 in.
Row space	0.025 in.
A	5 in.
B	6 in.
H	1.88 in.

The values for the contact width were divided in half because of symmetry and used in equation (5a) to get the resulting radial deflection. The radial deflection data was

averaged after taking several sets of half contact width readings for each durometer. These values were then plotted on a log-log scale against the effective nip load. The experimental nip load was determined from the pressure applied by each cylinder and multiplied by the area of the cylinder. The force displaced by the cylinder was confirmed by placing a scale under each cylinder during loading. The effective nip load is then determined by adding the forces and dividing by the length of the nip. The theoretical effective nip load, equation (7) is then determined by using the radial deflection. These plots are given in figure 4-2
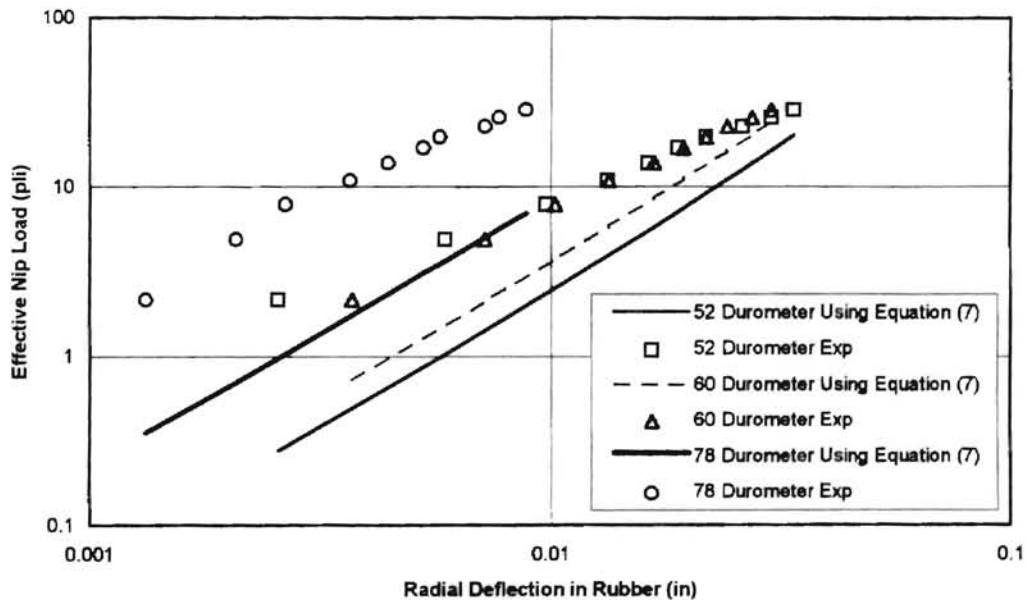
Figure 4-2: Variation of Calculated and Measured Effective Nip Load, Radial Deformation Calculated

The experimental values did not show distinct correlations, especially at the 78 durometer

In order to determine the source of error, equation (5a) was investigated. A non-contact displacement measurement system was used. The system utilizes an inductive technique to monitor the position of a target in relation to the sensor. An electromagnetic

field radiates out from the sensor. When a conductive target enters this field, a current flow is induced and produces a secondary opposing field. This opposing field reduces the intensity of the original field. An impedance variation in the sensor results. As the target moves the impedance changes. The impedance changes are converted to analog voltage. This voltage is directly proportional to the displacement of the target. Thus the output of the system is the displacement of the target.
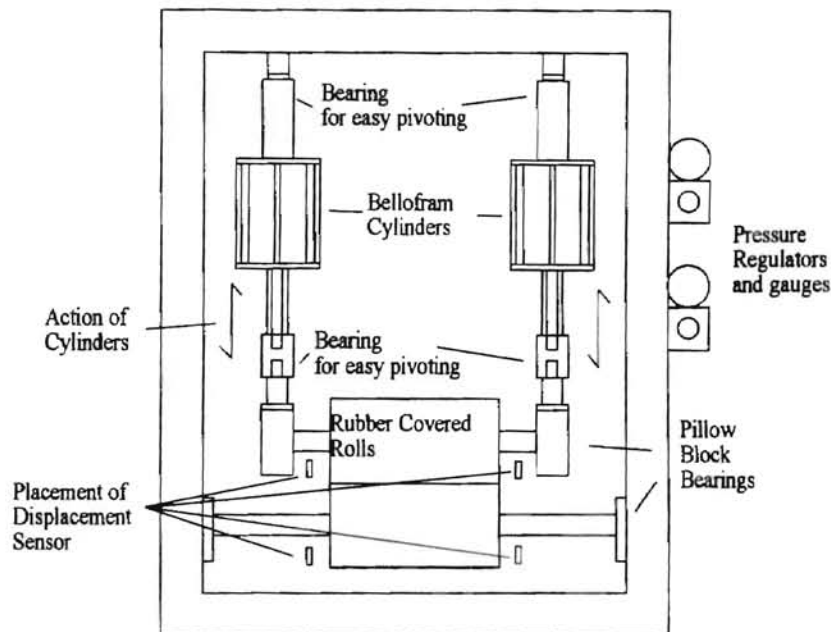
Figure 4-3: Illustration of location of displacement sensor

The specific instrument used was the Kaman KDM-7200, model 1U1. The measuring range was .040 inches. The minimum offset was .006 inches. This was the initial distance between the sensor and the target. The sensor required that the target material be nonmagnetic for great stability and linearity than magnetic material for readings. Aluminum in particular is a good material to use for the target. The resolution of the sensor is .000004 in.

The sensor needed to be used to detect the radial deflection of the rubber rolls in contact. The sensor was placed between the rolls underneath the outer flange of the rolls

as shown in figure 4-3. The sensor mounts to a lateral precision adjustable table. This table moves laterally by turning the adjustment knob. Each rotation of the knob moves the table by 1 mil (.001"). The location with respect to the test bed is shown in figure 4-4.
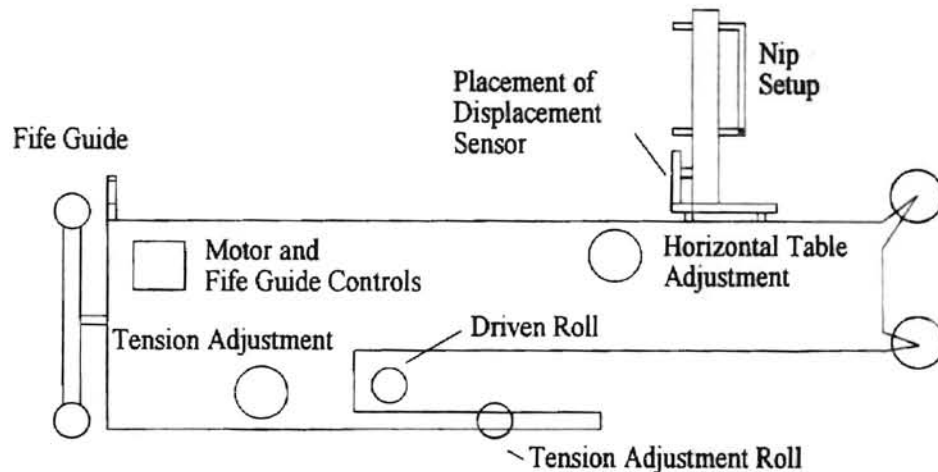
Figure 4-4: Location of displacement sensor overall view

After installing the sensor in the desired location., the sensor is offset and calibrated. The sensor is retracted by 40 mils (.04 in.) using the turning knob. The deflection of the 78 durometer rolls was less than 40 mils. For the other two sets of rolls, the sensor needs to be retracted during loading because the deflection of the rubber is greater than 40 mils. Therefore, when the nip was loaded the sensor would be offset when the displacement neared 40 mils before the experiment was complete. In these cases the final displacement is a summation of each retraction made till the rolls reached the maximum deflection at the highest loading. The readings were taken by incrementally loading the nip by 3 psi to a maximum of 30 psi. The sensor was also used to detect the deflection of the bottom roll due to loading where indicated. The deflection of the bottom roll was small compared to the sensor's full-scale reading. Therefore, no retractions of the sensor was needed. Having only one sensor, readings were taken on the left side of the

nip and the right side. The deflection of the bottom roll was subtracted from the

deflection of the top rolls. The values from the left and right side were averaged..
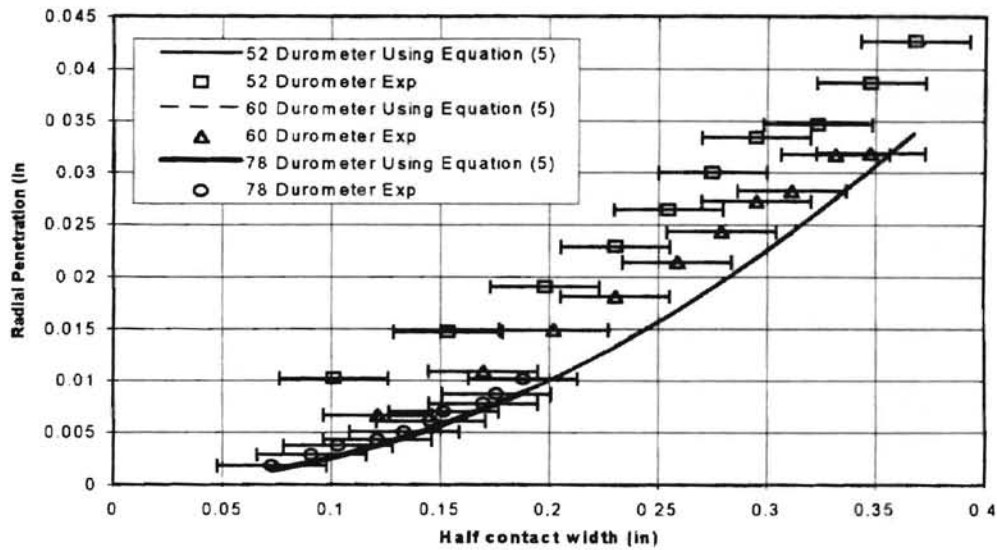
Figure 4-5: Comparison of measured and calculated radial deflections
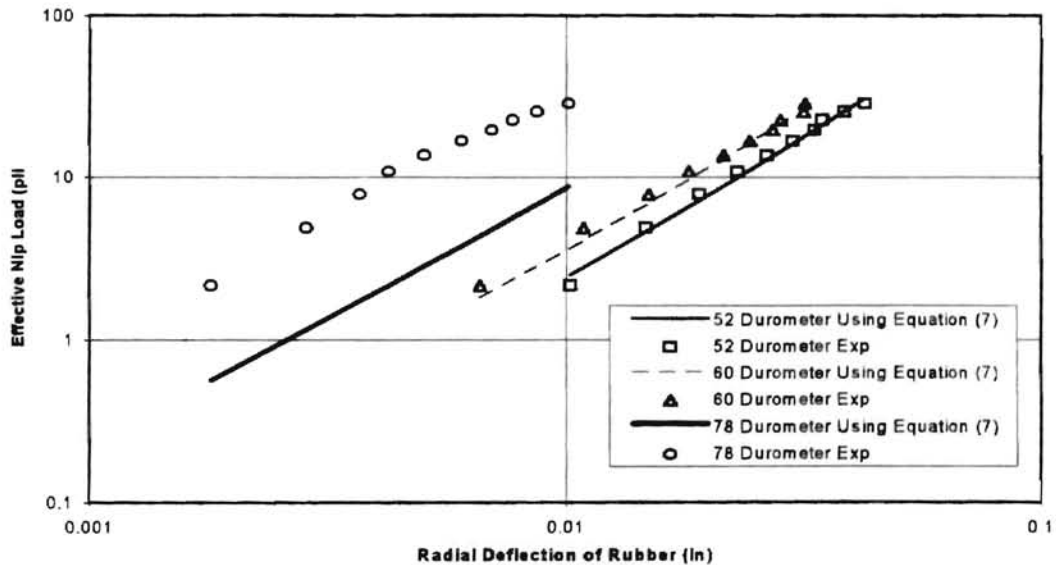
Figure 4-6: Variation of calculated and measured effective nip load, radial deformation is measured

The average values obtained were compared to the radial deflection calculated

from the equation (5a) that is related by the half width. The values are comparable as

shown in figure 4-5. The error bars indicate the distance between the force sensitive

resistors along the width of contact. Error bars would exist for in the vertical direction in

figure 4-5 for the resolution of the displacement sensor, however, the values would be very small, .000004 in. The values obtained were used in the equation (7) and the results are shown in figure 4-6. The measured values give a better correlation between the experimental data with the theoretical. The lack of correlation for the 78 durometer still remained.

The poor correlation of the rolls of 78 durometer hardness was investigated in detail. The first focal point of this investigation was the equation developed by Shelton which relates Young's modulus to the durometer and shape factor of the rubber.

$$E_a = 31e^{.048A}\left[1 + 1.7S^{(2.0-.004A)}\right] \qquad (4)$$

The shape factor is a ratio of loaded area per force free area [3]. Modulus tests were done on the pieces of rubber of the same material and durometer that were made at the same time the rolls were covered. The pieces of rubber were machined down to the same size. The pieces were constrained on four sides and a load was applied by an indentor as shown. Multiple indentors of various sizes were used to give different shape factors.
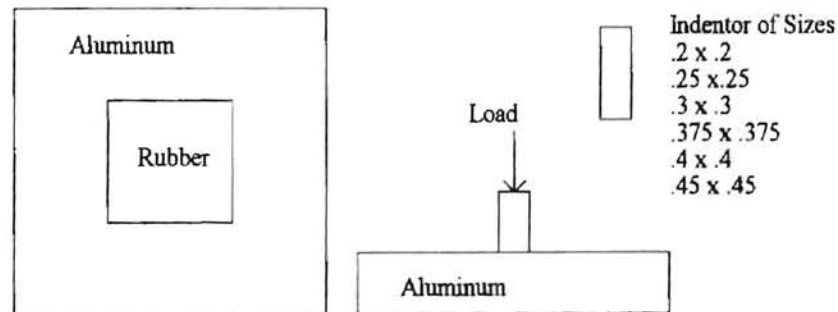
Figure 4-7: Illustration of rubber pieces confined for modulus testing

A plot of the modulus versus the shape factor was made. This plot was compared to the equation (4) developed by Shelton. In truth none of the 3 materials tested correlated very

well with equation (4). These are difficult tests to set up, however, and a great deal of
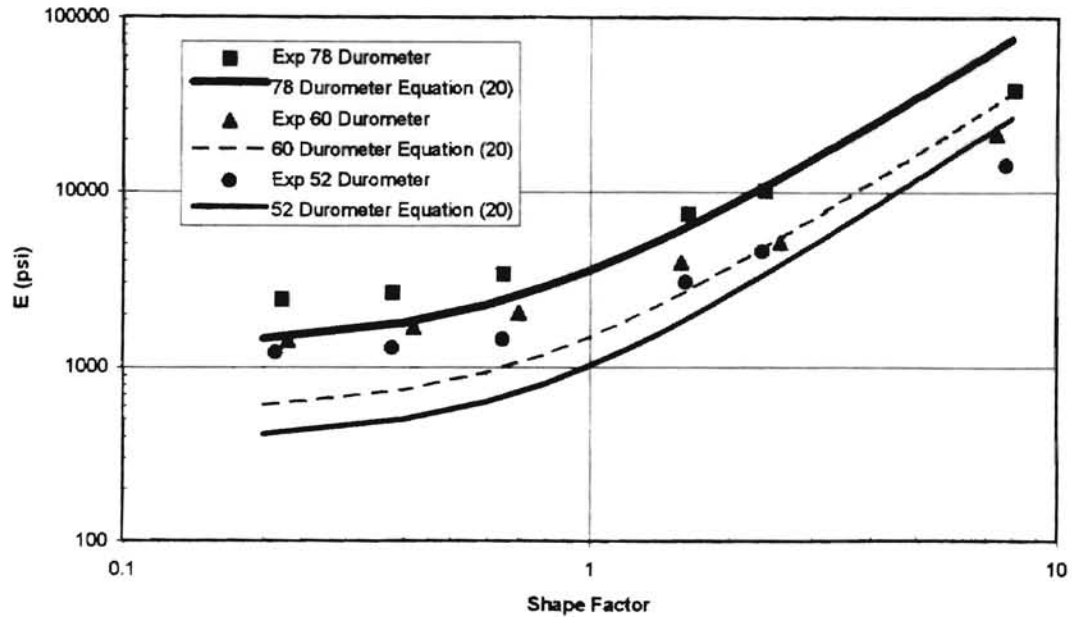
Figure 4-8: Modulus comparison at different shape factors

experimental error may be present. The trends are correct in that the modulus increases

with respect to durometer and shape factor as seen in figure 4-8.

Discrepancy remained for the 78 durometer. The modulus is approximately half of

theoretical.

Table 4-1: Compression modulus and k values for several durometer

IRHD	E(psi)	k	Bulk Modulus(psi)
30	130	0.93	142000
35	168	0.89	142000
40	213	0.85	142000
45	256	0.8	142000
50	310	0.73	146000
55	460	0.64	154000
60	630	0.57	163000
65	830	0.57	171000
70	1040	0.53	180000
75	1340	0.52	189000

Lindley [8] had developed equation (1) that calculated the effective nip load. In this equation, k had to be determined empirically from many samples by using equation (2). Using values from table 4-1 [1], the k factor was determined for the three rollers used in this investigation. Equations (22) and (23) are curve fits for the modulus of elasticity ,E, and k in table 4-1. Equation (1) was then used with the radial deflection data collected from the non-contact displacement sensor.

$$E = 26.549e^{0.0524A} \tag{22}$$

$$k = 1.07x10^{-5} A^3 - 1.6x10^{-3} A^2 + 6.52x10^{-2} A + 0.118 \tag{23}$$
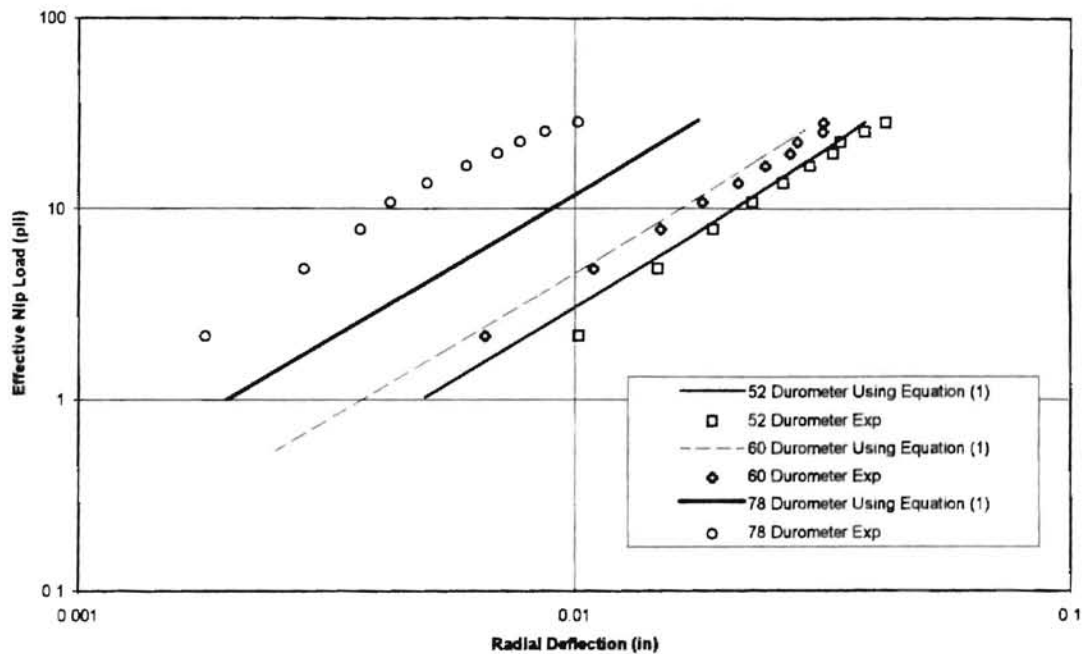
Figure 4-9: Variation of calculated and measured effective nip load using equation (1)

This plot was similar to the plot developed by equation (7). Therefore, equation (7) developed by Shelton could be used for calculating the effective nip load for rubber covered rolls of known initial radius, rubber thickness, and radial deformation. The discrepancy for the 78 durometer roll still remained.

Good and Markum [5] did a separate investigation in the modulus of the 78 durometer. They took the rubber covered rolls and placed them in diametral compression in a materials testing system. The values obtained were compared to the deflection data produced by the inductance probe. The results yielded are given in figure 4-10. The data points yielded by the probe were comparable to the data Good and Markum obtained.
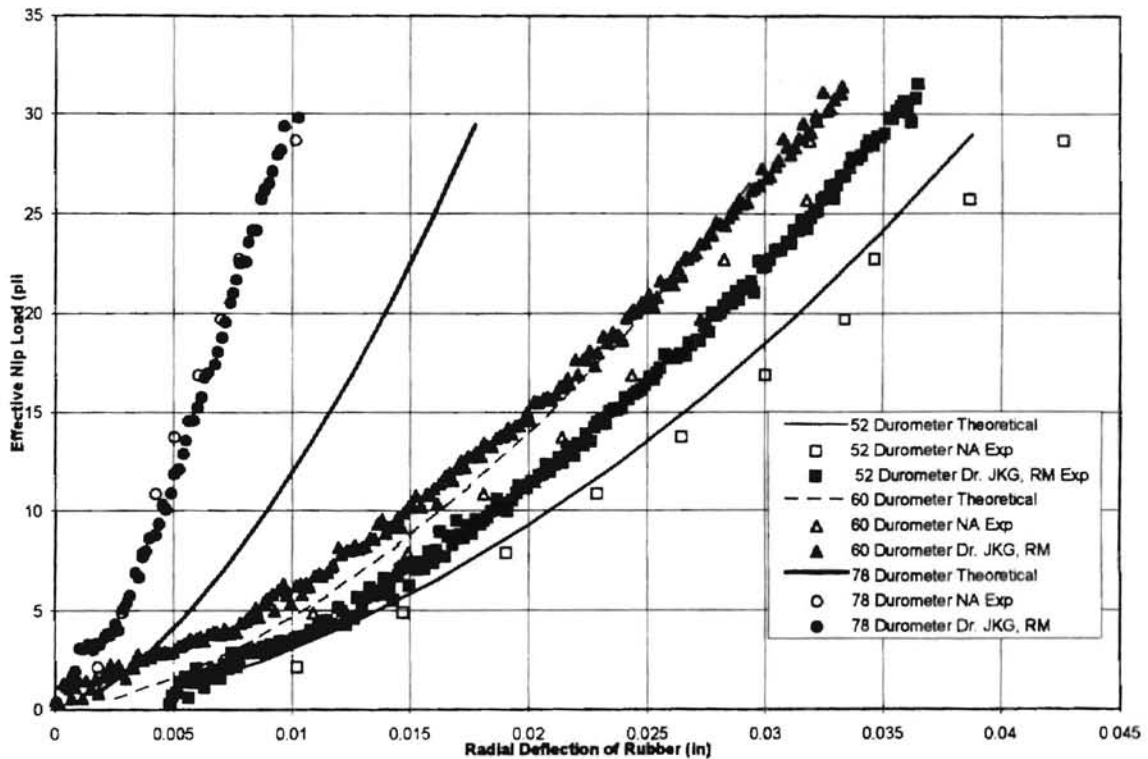
Figure 4-10: Variation of calculated and measured effective nip load,
Good and Markum results included

The theoretical curves also plotted were comparable for the 52 and 60 durometer rolls as with other rolls, but the 78 durometer roll's theoretical curve was approximately twice as much as that obtained from testing. The same procedure was done for other rolls around the WHRC. The test procedure worked well for all the rolls except for the 78 durometer roll. Note that a roller with a 76 durometer compared quite well to theory as well as a roller with a 72 and 79 durometer cover. Thus there is no indication that the theories

purported by Lindley and Shelton are in error for rollers with hard covers. Of all the rollers tested, only the 78 durometer rollers correlated poorly to theory. The design data for all of these rollers are contained in Appendix A. Although the theories seem reasonably robust there is evidence from the 78 durometer roller that Young's modulus may be a function of more variables than durometer and shape factor. If the manufacturers of these rolls would specify Young's modulus rather than durometer, which is the standard, the mechanical properties would be known without the need to divulge proprietary chemical properties. The manufacturer has explained there were no manufacturing differences in the roll except for the coloring. Fibers or other fillers were not present in the material that would increase the modulus of the material.
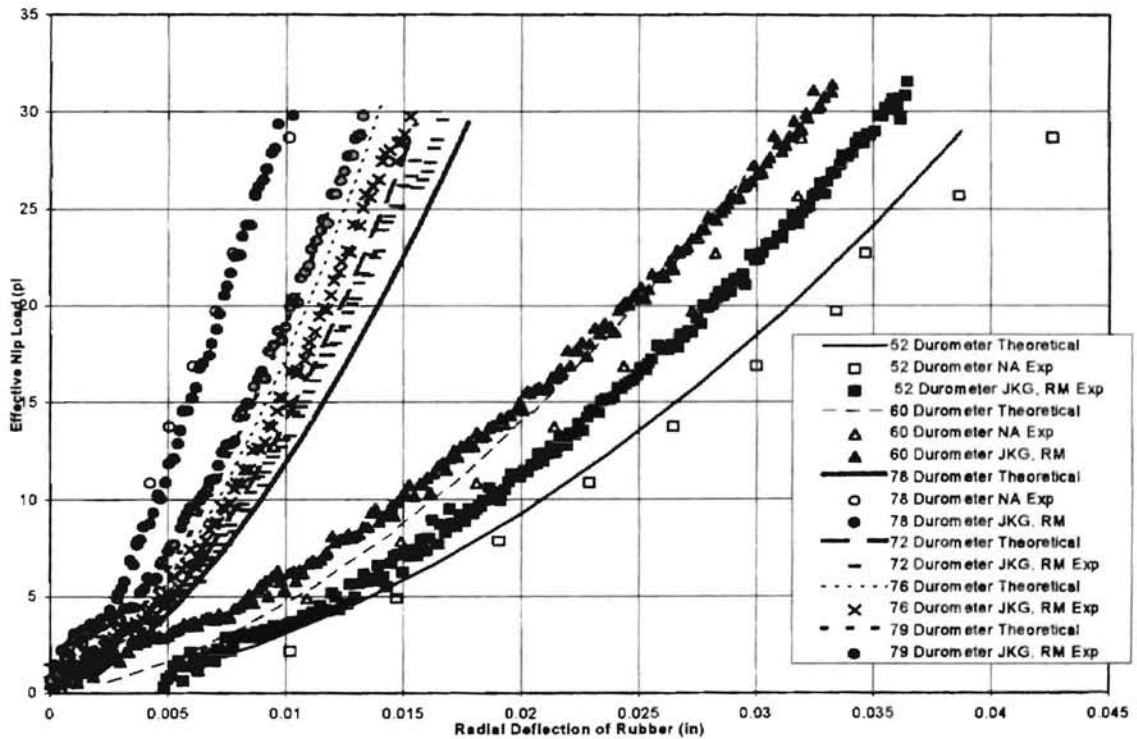
Figure 4-11: Variation of calculated and measured effective nip load, Good and Markum results of other 70+ durometer rolls

Equation (7) developed by Shelton to calculate the effective nip load at corresponding radial deflections of rubber covered rolls was verified for the 52 and 60 durometer rolls. The radial deformations of the rubber covered rolls were experimentally determined from a non-contact displacement sensor. A comparison between the calculated nip load and the experimental nip load is shown in figure 4-6. There was a lack of correlation for the rolls with the 78 durometer covering. An investigation of equation (4) was done to determine the poor correlation. This investigation only proved the trend of equation (4) to be true. Lindley's equation for effective nip load was used. Equation (1) was developed independently. Applying the radial deflections to this equation resulted in similar results as equation (7) shown in figure 4-9. Good and Markum also did an investigation to verify the theoretical equations. They used several rubber covered rolls at the WHRC. Their investigation data correlated well with the theories developed by Lindley and Shelton shown in figure 4-11. Their investigation showed the theories worked well with hard covers of 72, 76, and 79 durometer. Young's modulus for the 78 durometer rubber may be a function of more variables than hardness and shape factor. The theoretical equations worked well and could be used for further investigations.

Chapter V

Experiment ΔV/V and Y

After verifying the effective nip load equation, the strain at the edges of the web needed to be determined. Using equation (20) for difference in velocity per unit velocity was used. Verifying this equation gives an effective solution to determine the strain at the edges of the web.

Foreman [11] determined that more web had passed through the nip after one revolution of the nip than would be associated with the circumference of the nip rolls. He thereby deduced that the roller coverings were moving faster when passing through the nip contact zone than they were when not in contact. It is assumed that the web achieves the velocity of the rubber covering in the contact zone such that an accurate measurement of web velocity is also a measure of the velocity of the constricted rubber covering. This velocity should be greater than the velocity of the rubber covering away from the contact zone. In order to determine each of these velocities, encoders were used. These were Gurley Teledyne encoders that emit 10,000 pulses per revolution. Their output can be monitored with an HP Frequency/Counter such as Model 5314A. Placing a disc of known diameter on the shaft allowed for placement tangential to the rotating surface. One encoder was placed to record the velocity of the rubber covered roll as shown in figure 5-1. The other was placed on the driving roll to register the velocity of the web. The
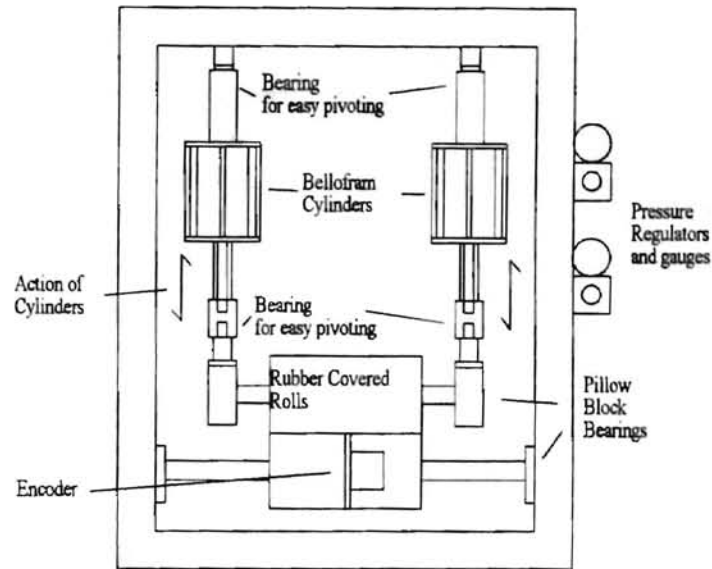
Figure 5-1: Placement of encoder to find the velocity of rubber covered rolls

placement with respect to the test bed is shown in figure 5-2. The controller for the DC

motor turning the driving roll was set for constant voltage, therefore constant velocity.

The nip was loaded incrementally by 3 psi from 3 to 30 psi equally on both sides. The

counter read the frequency output from the encoders and averaged 100 readings. These

readings were taken for each set of nip rolls.
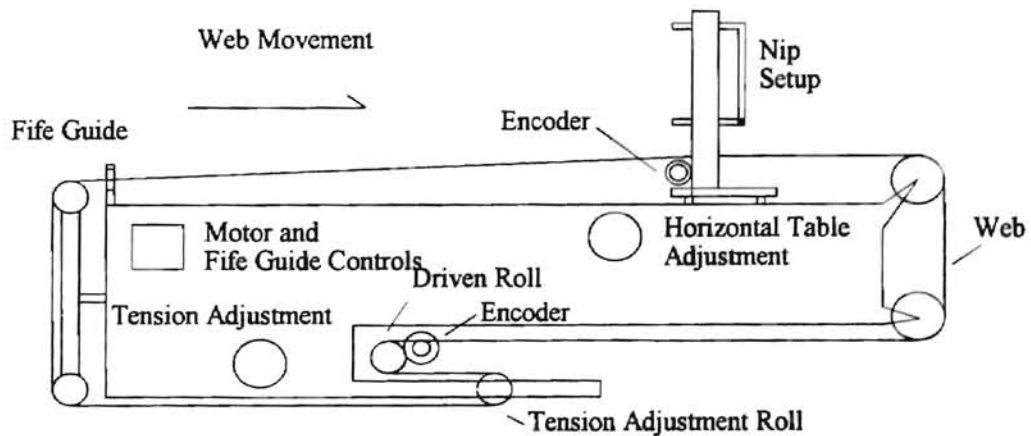
Figure 5-2: Location of encoders on test bed

The data was compared to the plot generated by equation (20) in figure 5-3.
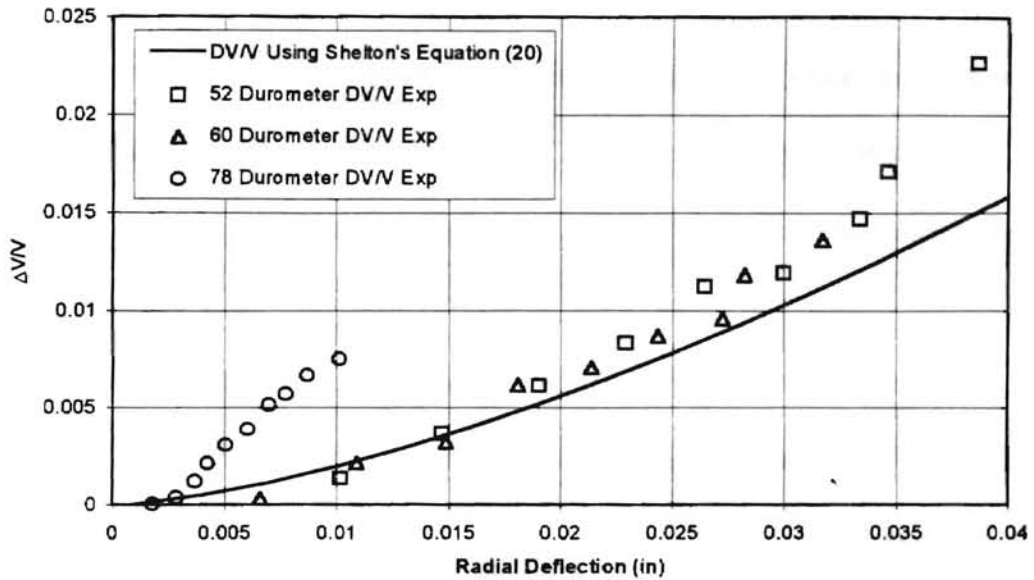
Figure 5-3: ΔV/V at corresponding radial deflection

The experimental data follows the theoretical plot quite well for the 52 and 60 durometer

rolls. The 78 durometer roll, however, does not. This would confirm that the behavior of

this roll is not as predicted as stated earlier. If the roll had behaved as predicted then the

strain plot would look similar to the that given in figure 5-4.
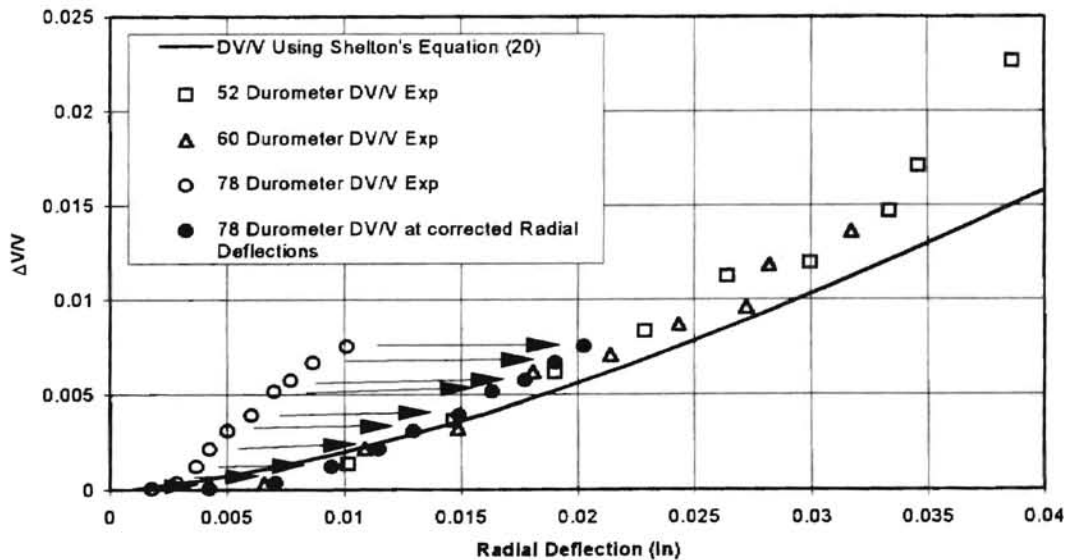
Figure 5-4: ΔV/V at corresponding radial deflections, 78 durometer adjusted

By obtaining the theoretical values for radial deflection, δ, from equation (1) or (7) and using the experimental values of strain, the corresponding plot of strain versus radial deflection would be similar to that of equation (20). Thus if a roller cannot be modeled by either equation (1) or (6), equation (20) would not model the it strain versus radial deflection behavior well.

Strain at the edges of the web determines the lateral deflection of the web. In order to quantify the deflection of the web, a 3M edge sensor was used. This sensor uses a laser to detect the edge of the web. By using a counter board in a computer, a LabView program tracks the edge of the web from the signal output by the sensors. Any small displacement in the web registers on the screen, to a resolution .001in. The sensitivity of the laser can be adjusted by calibrating the sensors over a specific range. The program also allows the user to adjust the average of the readings by adjusting the time period and the number of samplings taken.
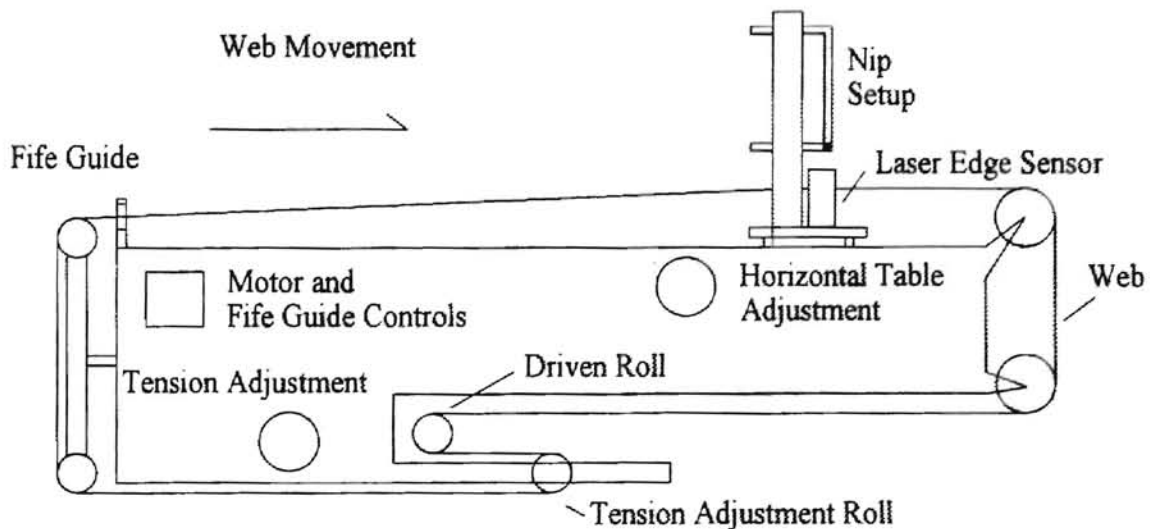
Figure 5-5: Location of 3M edge sensor in location

The laser was placed a few inches downstream from the nip as illustrated in figure 5-5. Since the maximum lateral deflection occurs at the nip, the web would remain in its

maximum deflected state till it returns to the Fife guide. The laser was placed so that the web in its undeflected state would cover about half the length of the laser. Calibrating the sensor here allows the laser to be sensitive over a half inch. The adjustment for the averages taken by the program were made so that they would cover one complete cycle of the web.

Three sets of data were taken for each set of rolls. The web was centered in the nip. Again the web width and thickness were 6 and .002 in., respectively. The web tension was 5.4 lb. The tension was verified by placing known weight on one end of the web and checking the displacement of the spring. The loads applied started at 24.9, 49.86, and 74.79 lb. The nip was first evenly loaded and then incrementally increased by .83 lb. on one side. Data was collected at each increment.

Figure 5-6: Lateral deflection at corresponding differential nip load

36
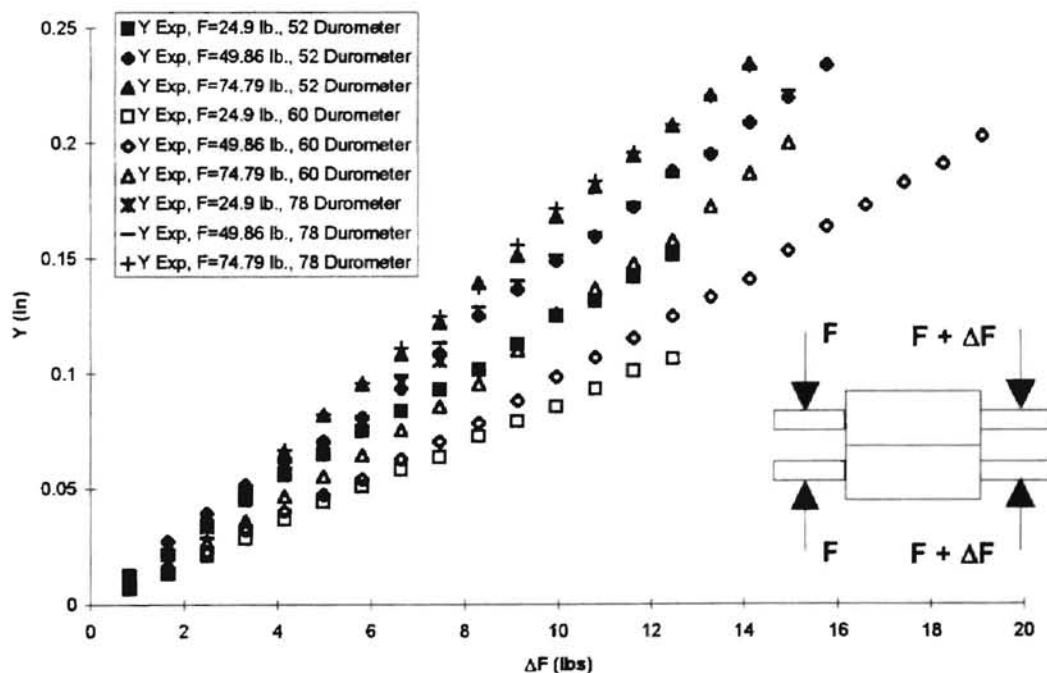
Data was taken till either separation between the rolls were visible on the lower loaded side or slackness was visible. The procedure was done for both sides of the nip. The data was then averaged. The data produced is given in figure 5-6.

The upper limit of the data is the critical point where slackness occurs. Using Good's equation (21) to determine this point is helpful. As stated earlier the center of the entering span into the nip behaves similar to the rotating roll. By entering the properties of the web into equation (21) and using only half of the entering length, the critical angle for the Polyester web is .004 radians. By modeling the web as a beam with two rigid supports and a half-length equal to the length of the entering span, the maximum deflection can be found in terms of rotation angle.

$$\theta_{max} = \frac{1}{64}\frac{PL^2}{EI} \text{ and } P = \frac{192YEI}{L^3}$$

$$Y_{cr} = \frac{\theta_{cr}L}{3}$$

After making the substitutions, the critical deflection was .211 in. For this type of web at the length used this is the maximum deflection of use by the lateral deflection equation.

In order to verify the lateral deflection equation, a spreadsheet was incorporated to find the theoretical deflection. The spreadsheet was setup to input the forces applied on either side of the nip, the durometer of the rolls, and the initial thickness and radius. By modeling the nip as a beam, the reaction forces were found at the edges of the web and therefore the effective nip load. This is given in Appendix B. Once the effective nip loads were determined at the edges of the web in the undeflected state, the effective nip load equation was driven to equal the determined effective nip load by using the solver function. Solver changed the radial deformation till the two set of effective nip loads were

equal. Figure 5-7 gives a flow chart that illustrates the spreadsheet analysis. Using the

radial deformation
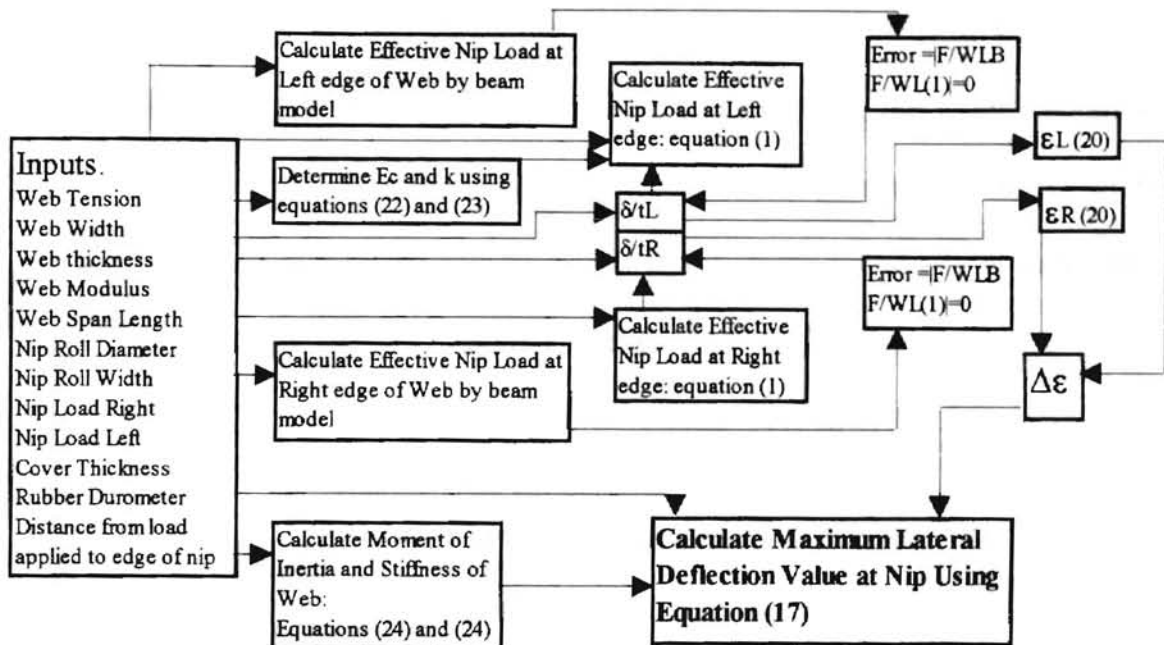
Figure 5-7: Flow chart of spreadsheet operation to calculate maximum lateral deflection

at the edge of the web, the strain was solved. The difference in strain of the edges was

used in equation (17). Equations (24) and (25) were used to calculate the inertia and

stiffness of the web respectively [7].

$$I = \frac{tW^3}{12} \qquad (24)$$

$$K = \sqrt{\frac{T}{EI}} \qquad (25)$$

The lateral deformation was then solved. Examples of the spreadsheet calculations are

given in Appendix B. Figure 5-8, 5-9, and 5-10 show the point of the calculations given in

Appendix B. This was done for each set of data.

The lateral deformation data correlated well with the theoretical data except for

the 78 durometer rolls shown in figures 5-8, 5-9, 5-10, 5-12, 5-13, and 5-14. Excellent

correlation exists for the 24.9 lb. base level load. The maximum difference for the other

two base level loads are approximately .05 in. for the 49.86 lb. And .08 in. for the 74.79

lb. This is relatively small. For the data that corresponds lateral deflection, Y, with the

change in force, ΔF, the trends of the experimental data is opposite that of the theoretical

data. As the base level loads increase the theoretical lateral deflection decreases while the

experimental lateral deflection increases. However, the graphs generated that shows the

lateral deflection at the corresponding radial deflection, δ, the trends are the same. The

dispersion of the experimental data, however, is greater than that of the theoretical

prediction for all cases. This indicates the model is less sensitive to load levels compared

to the experimental data.
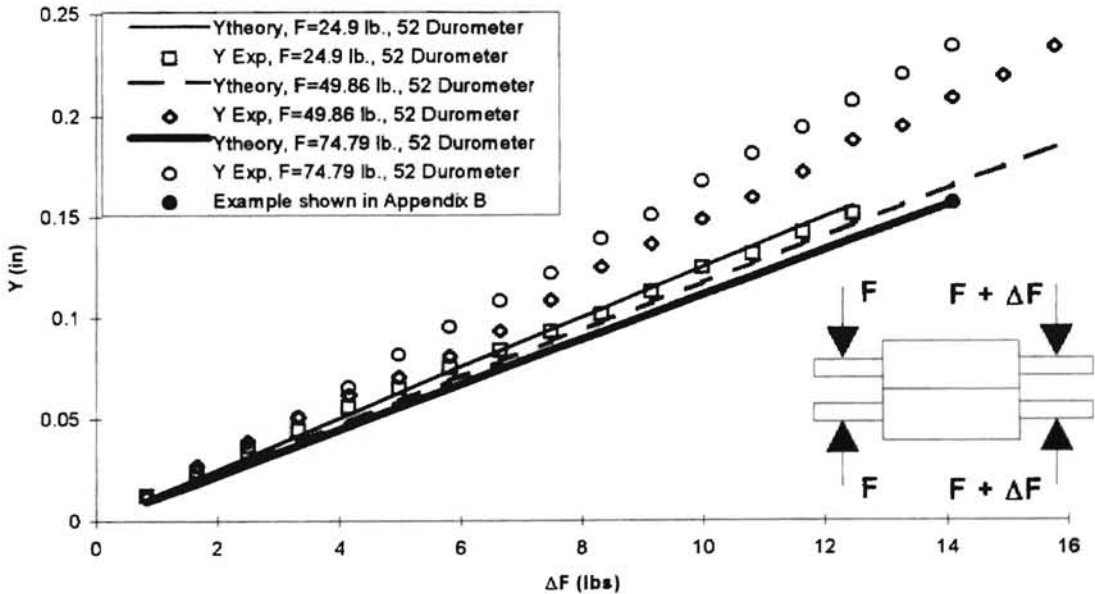
Figure 5-8: Theoretical and experimental lateral deflection at corresponding differential nip load, 52 durometer
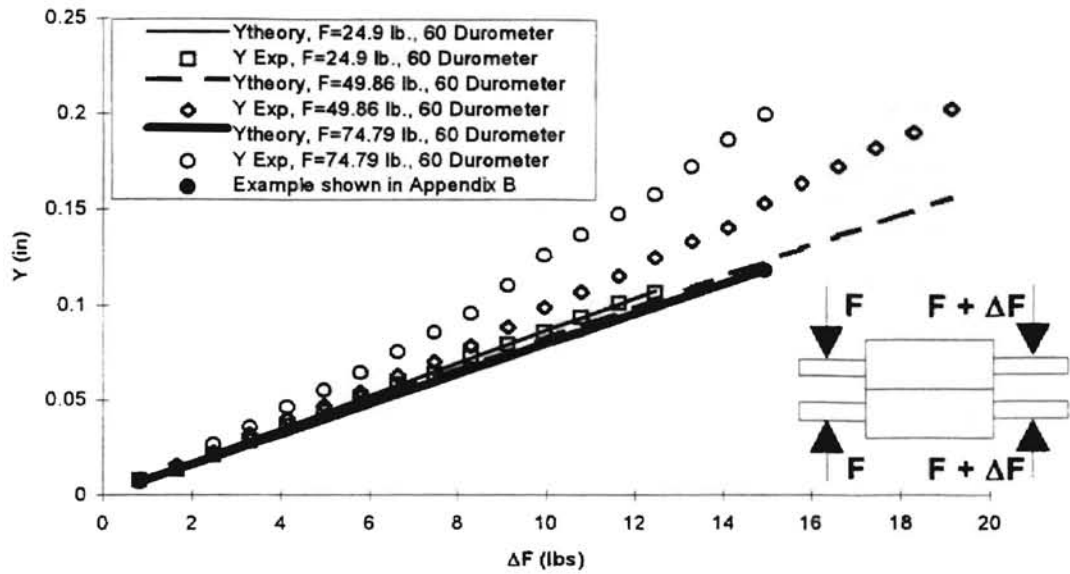
Figure 5-9: Theoretical and experimental lateral deflection at corresponding differential nip load, 60 durometer
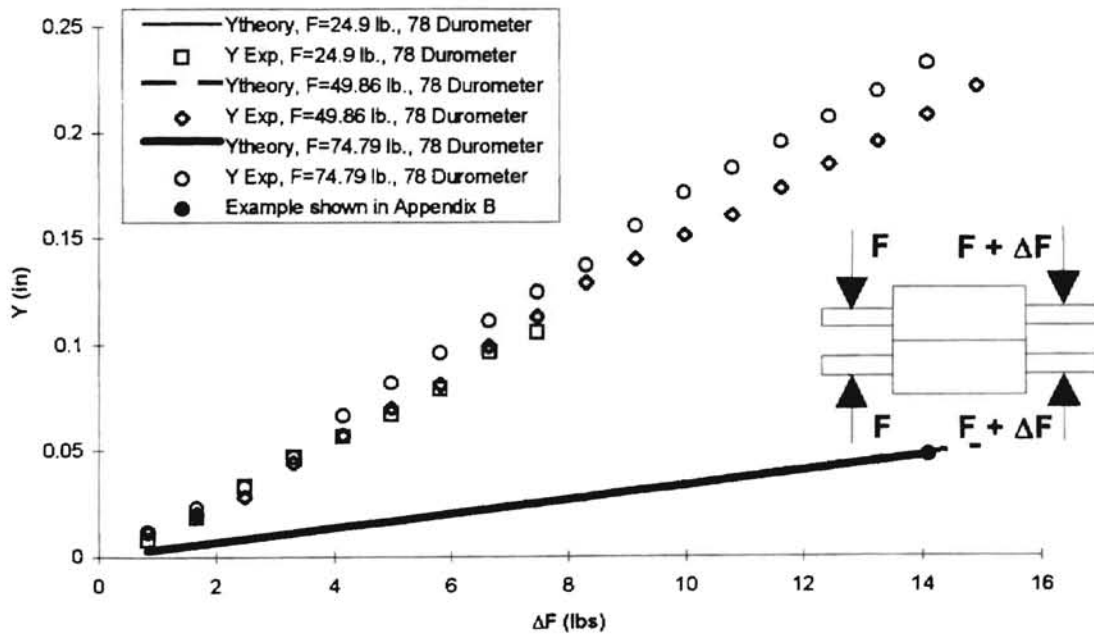
Figure 5-10: Theoretical and experimental lateral deflection at corresponding differential nip load, 78 durometer
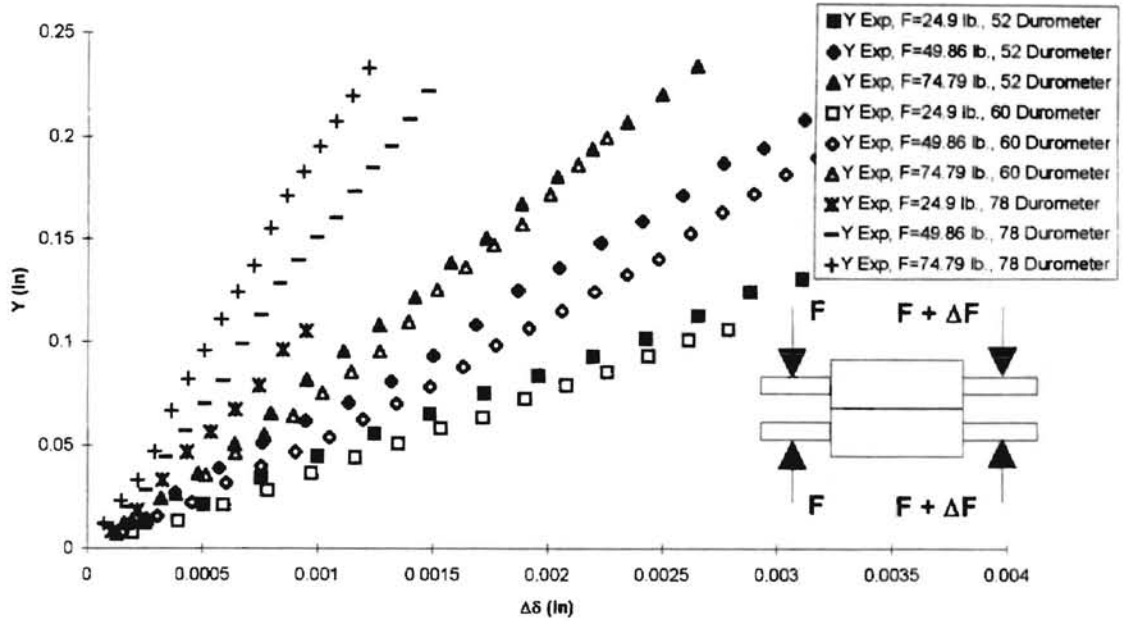
Figure 5-11: Lateral deflection at corresponding differential radial deflection of rubber covering
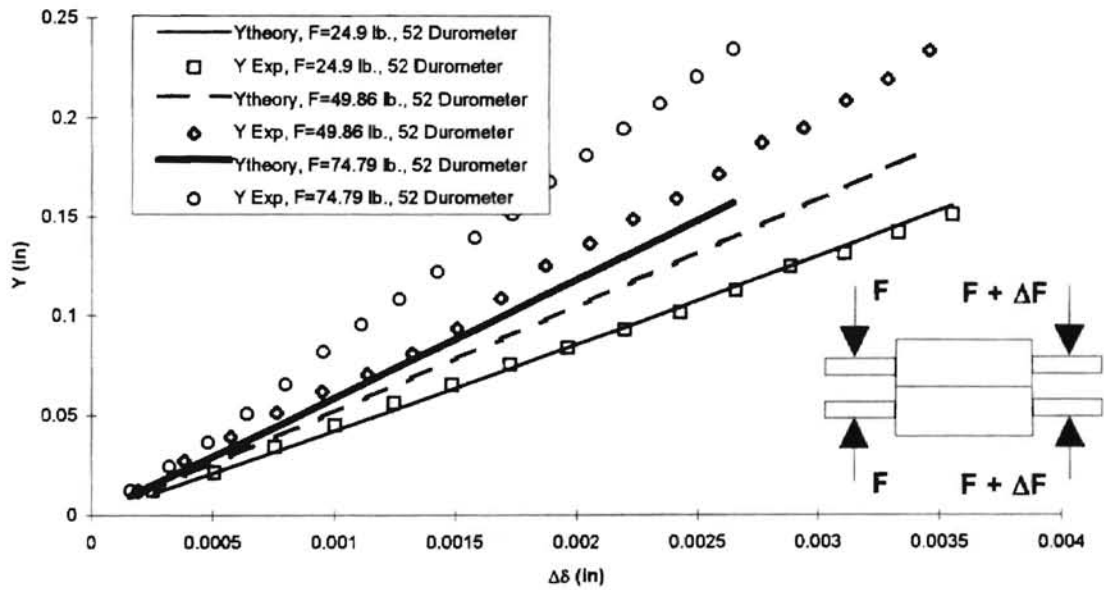
Figure 5-12: Theoretical and experimental lateral deflection at corresponding differential radial deflection, 52 durometer

41
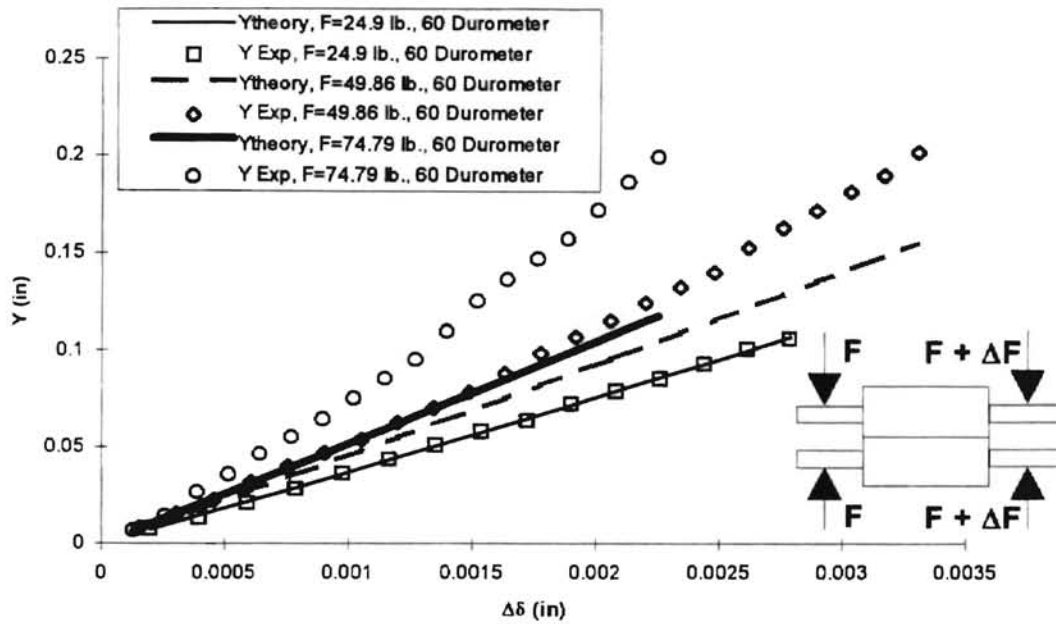
Figure 5-13: Theoretical and experimental lateral deflection at corresponding differential radial deflection, 60 durometer
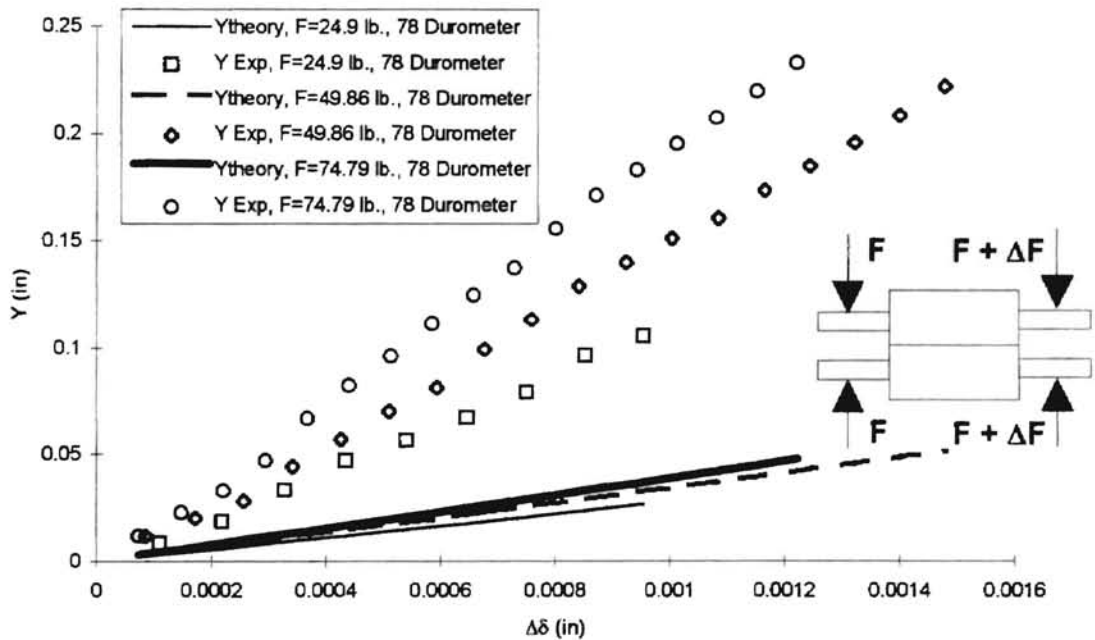
Figure 5-14: Theoretical and experimental lateral deflection at corresponding differential radial deflection, 78 durometer

In an attempt to resolve the dispersion difference between the theoretical and experimental data, the effective nip loads were found at the corresponding location of the

42

deflected web. When the new lateral deflection was found for the loads at this point, there was no change from the previous theoretical deflection. Therefore, the deflection of the web does change the effective nip loads at the edges of the web, but the change in stain and lateral deflection was not effected.

In applying the results from this study in design of web lines, one must consider a few points. The selection of durometer of the rubber is critical. As seen in figure 5-6, lateral deflection of the web is larger for the same differential nip load for the lower durometer as compared to the higher durometer, discounting the 78 durometer rolls. The lateral deformation remains the same if the differential radial deflection is the same for all durometer as shown in figure 5-11. Also for consideration is the application of the rubber. For high nip loads, the lower durometer coverings may not be as reliable and prone to failure. The lower durometer coverings also have a shorter span of use. Thus higher durometer rolls may be required. This would then require a larger differential loading than for the lower durometer to achieve the same lateral deflection.

Equation (17) used to predict the lateral deflection of the web proved to be a useful tool to do so. Equation (20) was also verified as shown in figure 5-3 for the 52 and 60 durometer rolls. If the 78 durometer roll had conformed to either equation (1) or (7), which calculate the effective nip load, equation (20) would have predicted its strain behavior as shown in figure 5-4. Once equation (20) was verified the lateral deflection was found for each of the rolls for three different base load levels. The data was plotted against the incremental change in force in figure 5-6. By applying Good's equation (21) the upper useful limit of the data was found. By the use of a spreadsheet and a solver program the lateral deflections were found at the corresponding differential load levels.

The experimental data was plotted against the differential radial deflection for the three

different rolls in figure 5-11. This showed that for the same differential radial deformation

the same lateral deflection would occur. The experimental and theoretical data were

plotted against the differential forces, figures 5-8, 5-9, and 5-10, and the differential radial

deflections, figures 5-12, 5-13, and 5-14. The trends of the experimental data was

opposite that of the theoretical for figures 5-8, 5-9, and 5-10. The trends were, however

the same for the plots against the differential radial deflections. The dispersion was

greater between the experimental data than that of the model. The experimental data is

more sensitive to the load levels than the model. However, the correlation was good for

the 52 and 60 durometer cases. The 78 durometer was an anomaly. The equation for the

lateral deflection could be used for design applications.

Chapter VI

Conclusions

The objective of this research was to quantify and experimentally verify the lateral deformations of web due to non-uniform nip loading with rubber. Specifically, the equations developed by Shelton [11] for effective nip load, (7), and for lateral deflections of web, (17), were to be verified. Once verified these equations could be used for an innovative guiding mechanism and other web line applications.

For the verification of equation (7) for the effective nip load, a direct correlation of experimental data with equation (7) was shown in figure 4-6 for the 52 and 60 durometer and for 72 and 76 durometer shown in figure 4-11 The 78 durometer roll, however, did not correlate well. In pursuit of determining the difference, an investigation of equation (4) was attempted. Equation (4) was a curve fit of data that determines compressive modulus from shape factor and durometer. This investigation proved inconclusive only the trend of modulus to shape factor was verified Using equation (1) developed separately by Lindley [1] also showed the same correlation of experimental data with theory shown in figure 4-9. The 78 durometer roll remained an anomaly as shown in figure 4-9. Good and Markum's [5] diametral tests showed other rolls of different durometer resulted in data that verified the theoretical equations shown in figure 4-11. In equation (1), the factor "k" must be determined empirically from equation (2) which

calculates the compression modulus from Young's modulus, shape factor, and the factor

"k". The shape factor is determined from the original undeflected roll diameter, the

thickness of the rubber covering and the radial penetration of the roll. However, equation

(7) only requires the undeflected radius of the roll, the covering thickness, durometer, and

radial deflection of the roll. The compressive modulus and shape factor have already been

incorporated into equation (7). Equation (7) provides an effective solution to determine

the effective nip load for a given thickness, durometer, and radial penetration.

Once equation (7) was verified, it could be used to help determine the lateral

deflection of the web due to uneven loading. In order to verify equation (17), the strain at

the edges of the web needed to be determined. Thus, the verification of equation (20) was

required. Figure 5-3 showed good correlation between experimentally determined $\Delta V/V$

at corresponding radial penetration to a plot of equation (20) for the 52 and 60 durometer

rolls. If the 78 durometer roll had conformed to equations (1) or (7), it would have

conformed to equation (20) as shown in figure 5-4. Thus, equation (20) was used to

determine the strain at the edges of the web. Using this equation to find the change in

strain from one edge of the web to the other, the lateral deformations were then found.

Figures 5-8 and 5-9 showed reasonably good correlation between the experimentally

determined lateral deflection and the plots generated from equation (17) for the 52 and 60

durometer rolls against differential loads. Figures 5-12 and 5-13 showed good correlation

when the experimental and theoretical data was plotted against the differential radial

penetration. The difference between actual and theoretical was relatively small. The

equation for lateral deflection can be used for prediction, reasonably well, of displacement

of the web with known stiffness, entry length, and the difference in strain from one edge to the other of the web.

The experimental data obtained for lateral deflection corresponded well with the theoretical model formulated by equation (17) except for the 78 durometer roll as shown in figures 5-8, 5-9, 5-10, 5-12, 5-13, and 5-14. The data however did not fall directly upon the model. Only for the low base level loading did the data fall directly on the plot generated by equation (17). The lateral deflection increased with the higher base level loading. The model, however, predicted that the lateral deflection would decrease with the increased base level loading shown in figures 5-8 through 5-10 when plotted against ΔF. Similar trends would exist when the lateral deformations were plotted against $\Delta \delta$. The experimental data showed great dispersion between each base level loading for all the figures. The dispersion between each base level of the model was not as great. This indicates that the theory is less sensitive to the load levels as compared to the experimental data. For the same ΔF greater lateral deflections exist for lower durometer covering. For the same $\Delta \delta$, however, lateral deflections are equal for any durometer covering. The correlation between the experimental data and the theoretical model is good and useful for design.

Future Work

Further investigation of the strain equation, (20), would be beneficial. This equation was curve fit by Shelton from the data provided by Foreman. Foreman assumed that the web achieves the velocity of the rubber rolls in the contact region. The velocity in this region should be greater than the velocity of the covering away from the contact zone.

An accurate model and basis for this greater velocity could provide a more accurate equation for strain.

An investigation of modulus could also be useful. After investigating the 78 durometer roll, Young's modulus may be a function of more variables than durometer and shape factor. Young's modulus may also be a function of the composition of the rubber. A better understanding of the relationships effecting Young's modulus could yield a more accurate algorithm and may explain why experimental data and theoretical models yield different trends as shown in figures 5-8 and 5-9.

Research could also be performed on the small deflection assumption of the rubber covered roll. Being able to determine the point where this assumption does not apply could be useful in predicting the lateral deflection of the web. This could give a more accurate description of lateral web movement.

The effect of friction between the rollers and the web would also be interesting. Early works on the first experimental setup showed that a metal roll in contact with a rubber covered roll may yield no lateral movement. Thus the coefficient of friction between aluminum and pet must have been larger than that between pet and nitrile rubber. Even when the rollers are similar but with low coefficient of friction one must wonder if the web achieves the maximum velocity of the rubber in the contact zone. This investigation could show a relationship between friction and lateral web movement.

Once the equations for lateral deflection and effective nip load have been refined, they could then be used for web guiding. By using an edge sensor and feedback controller, the nip setup could be used as a web guidance system.

Also with a verified equation for lateral deflection a third derivative with respect to x would yield shear which has been shown to be a primary variable in predicting web wrinkling. Thus, equations such as equation (20) could be used with the understood restrictions of a slack edge [6] or that wrinkling may occur at some critical value of lateral deflection.

Recovery effects of the rubber covering may also have an impact on lateral deflections of the web. Some rubber covering materials may not recover from radial deformations as quickly as others. The effect of this may be adverse for this study. Recall expression (20), if δ does not recover to zero in the time required for the rubber covering to reenter the contact zone then less strain within the web material can be expected. The nitrile material used in this investigation was relatively quick to recover from deformations which was proven during upload and download testing when verifying the load, F, versus deformations, δ, expressions (1) and (17). This effect can occur in other elastomers. An in-depth study can be made in this area to study the effects of different covering material.

REFERENCES

[1]   Allen, P.W., P.B. Lindley, and A.R. Payne. Use of Rubber in Engineering, Maclaren and Sons Ltd, London, 1967.

[2]   Batra, R.C. "Rubber Covered Rolls - The Nonlinear Elastic Problem." Transactions of ASME, Vol. 40, March, 1980, pp. 82 - 86.

[3]   "An Engineer's Guide to Natural Rubber." Materials Engineering, April, 1970, pp. 22 - 84.

[4]   Foreman, A.R. "Application Rubber Covered Rolls to Pinch Rolls and Bridles." Iron and Steel Engineer, August, 1964, pp. 111 - 120.

[5]   Good, J.K., and R. Markum. Informal Test of Nip Cover Deformation due to Diametral Compression, 1996.

[6]   Good, J.K. "Multispan Wrinkling in Web Lines." Paper presented at the Semiannual Technical Review and Industry Advisory Board Meeting, Tab No. 12, October, 1996

[7]   Juvinall, Robert C. and Kurt M. Marshek. Fundamentals of Machine Component Design. 2nd Edition, John Wiley and Sons, New York, 1991.

[8]   Lindley, P.B. "Load-Compression Relationships of Rubber Units." Journal of Strain Analysis, Vol. 1, No. 3, pp. 190 -195.

[9]   Miller, R.D.W. "Variations of Line Pressure and Rolling Speed with Indentation of Covered Rolls." British Journal of Applied Physics, Vol. 15, 1964, pp. 1423 - 1435.

[10]   Parish, G.J. "Apparent slip between metal and rubber-covered pressure rollers." British Journal of Applied Physics, Vol. 9, November, 1958, pp. 428 - 433.

[11]   Shelton, J.J. Informal notes on web deformations due to nonuniform nip pressure, 1995.

[12]   Shelton, J.J. "Lateral Dynamics of a Moving Web." Ph.D. Thesis, Oklahoma State University, 1968.

Appendix A

Table A-1: Design data for diametral compression for tests of Good and Markum

Durometer	52	62	72	76	79	78
D (in)	3.9	4	2.75	2.75	4.71	4
t (in)	0.475	0.55	0.275	0.275	0.378	0.5
W (in)	8	8	8.5	8.5	7	8
E (psi)	396	672	1140	1409	1651	1565
k	0.68	0.57	0.53	0.51	0.51	0.51

The rolls designed specifically for this investigation are shaded in table A-1.
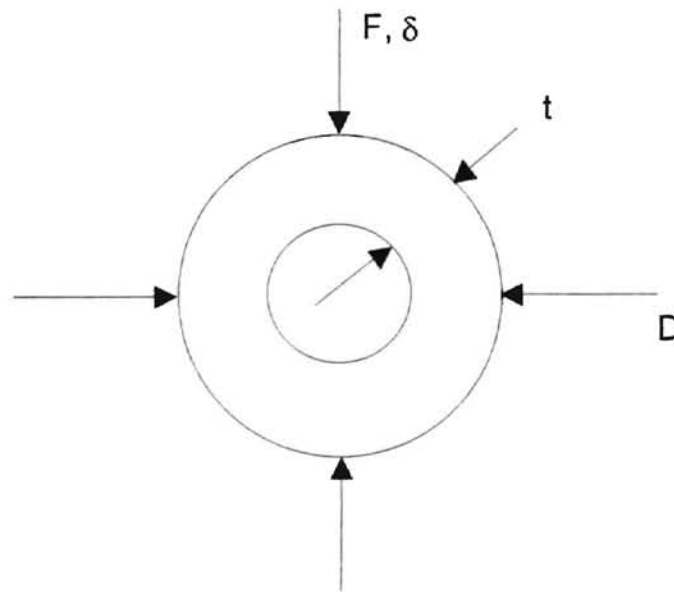
Figure A-1 Illustration of diametral compression of tests conducted by Good and Markum

Table A-2: Data collected from diametral compression, Good and Markum

| 52 Durometer		60 Durometer		72 Durometer		76 Durometer		79 Durometer		78 Durometer	
LOAD (pli)	δ (in)	LOAD (pli)	δ (in)	LOAD (pli)	δ (in)	LOAD (pli)	δ (in)	LOAD (pli)	δ (in)	LOAD (pli)	δ (in)
0.28511667	0.00483333	0.46209375	0	1.45155	0	0.5727606	0	0.65891529	0	0.96907941	0.000585
0.7001	0.00497	0.33394063	0.000145	0.58999412	0.00025	0.5038359	0.000168	1.43431647	0.0001675	1.64109294	0.00075
0.87097333	0.00515	1.34087938	0.0003325	1.14138882	0.0003525	0.6589153	0.00025	0.93461294	0.0003325	1.93402059	0.000855
1.37139458	0.00527667	1.21272563	0.0005	1.14138529	0.0005175	0.3659841	0.00044	2.20971765	0.0005	3.07127765	0.00102
1.65211583	0.00549833	0.57194375	0.00069	1.10692824	0.0006875	0.9690759	0.000563	1.77893824	0.0006675	3.05404412	0.0011875
0.602455	0.00563833	1.17610438	0.000835	0.77953	0.0008525	0.9173924	0.000793	2.45095471	0.0008125	3.27804647	0.001375
1.34698292	0.00583167	1.46904	0.00098	1.00354	0.001	1.2964712	0.00098	2.81280706	0.001	3.01958353	0.0016025
2.09151333	0.00597167	0.55363313	0.0011475	0.96907647	0.001185	0.8656918	0.001085	2.74388588	0.0011025	3.32974059	0.0017075
1.78638	0.00613833	1.46903938	0.0013125	1.05523118	0.00133	1.45155	0.001313	2.58880294	0.0013725	3.29528	0.001875
1.10287583	0.00630333	1.04795125	0.0015	1.65832	0.0014975	2.1063329	0.001478	3.15743176	0.0014975	3.62267176	0.0020825
1.5788875	0.00647	1.52396125	0.0016875	2.15802706	0.0016425	2.0029447	0.001645	3.55374706	0.0017075	3.81221471	0.0021875
2.01828	0.00687833	0.82825813	0.001835	2.12356294	0.0018525	2.0029447	0.00175	3.51928353	0.0018725	3.74329	0.0023325
1.8107875	0.00680333	1.670425	0.0020225	2.20971412	0.0019975	1.7444747	0.001935	3.60543824	0.00202	4.29468471	0.00264
1.60329708	0.00698333	1.890125	0.00221	2.91619529	0.002185	2.1752608	0.002123	3.43312882	0.002165	4.01898471	0.002665
2.27459417	0.00713667	2.3112075	0.002335	2.70941882	0.0023525	2.3820306	0.00231	3.55375059	0.00229	5.08731647	0.002895
2.06709917	0.00729	1.98166438	0.00248	2.72665235	0.0024975	2.7438824	0.002458	3.70882647	0.0024775	5.41470824	0.00304
2.84824667	0.00747	2.25628625	0.0026675	2.5888	0.002685	2.6232671	0.002603	3.95006353	0.002645	5.75933	0.003166
2.16474417	0.00765	1.83520063	0.002855	2.69218824	0.0028725	2.8817341	0.00273	3.72605353	0.0028525	6.87935235	0.0033925
2.372235	0.007775	1.57888688	0.00298	2.98511588	0.002935	3.1918924	0.002895	3.77775412	0.0029775	6.63811882	0.00354
2.87265833	0.00795667	2.10982188	0.0031875	3.08850412	0.0031225	3.3469712	0.003083	4.36360882	0.0031425	7.67198471	0.0037075
2.9092725	0.00817833	2.10981813	0.003335	3.39866529	0.0033325	3.3814347	0.00329	4.38084	0.003415	7.98491176	0.0038525
3.031325	0.00830333	2.80552875	0.00348	3.48482294	0.0034975	3.3986653	0.003478	4.44976412	0.003455	8.61969882	0.0039775
2.83604167	0.00844167	2.49428938	0.0036675	3.34697471	0.0036225	3.6398988	0.003645	4.39807	0.0036025	8.79200765	0.00425
2.88044875	0.00864833	2.64075688	0.0038325	3.34697471	0.00379	3.4848194	0.003793	5.20793471	0.0038325	9.34340882	0.0043925
3.15338208	0.00879	2.64075313	0.00402	3.63989882	0.003955	3.7949841	0.003935	5.38024765	0.0039975	10.2738888	0.00456
2.93368458	0.00898333	2.82383188	0.0041475	3.58821176	0.004145	4.1223724	0.004145	5.96610588	0.004145	10.0671165	0.004685
3.28322917	0.00913667	3.17169313	0.0042925	3.82944118	0.004395	4.3463759	0.00425	5.82825412	0.0043525	10.8942041	0.004895
3.00691792	0.00930333	2.82383563	0.00446	3.60543824	0.0045175	3.7432935	0.004458	5.93164235	0.00454	11.8763788	0.00504
3.4585175	0.00949867	2.93368563	0.004625	3.74329059	0.0046225	4.63931	0.004605	6.65534941	0.0047075	12.1003853	0.00525
3.20220125	0.009635	2.84214625	0.0047925	4.44976412	0.0049125	4.9494676	0.00475	6.82766235	0.00477	12.8757876	0.005415
3.4585125	0.00980333	2.9336825	0.005	4.32914882	0.0049775	5.2079312	0.004958	7.34459294	0.0050175	13.5478035	0.00552
3.40989375	0.00998333	3.18999688	0.0051875	4.70823059	0.0052075	5.0873165	0.00506	7.65475412	0.005145	14.5472082	0.0056425
3.5805725	0.010135	3.20830688	0.0053125	5.07009	0.0053725	6.0177966	0.00529	7.68921412	0.00529	14.5844382	0.0058525
3.64159583	0.01032833	3.33646438	0.0054575	5.31132294	0.0055375	5.4664053	0.00548	8.56800471	0.00556	15.2192212	0.00602
3.66600792	0.01051	3.59277438	0.0056875	5.17347118	0.005705	6.4141124	0.005605	8.94709	0.005665	15.7533859	0.0061875
3.69041958	0.01062167	3.44631063	0.005875	5.60425059	0.00581	6.6725829	0.00579	9.30894176	0.0058125	16.7527894	0.0063125
3.99555292	0.01078833	3.59277438	0.0059575	5.96610294	0.0060175	7.4479812	0.005958	9.58464176	0.0059575	16.9940265	0.0064575
3.87349375	0.01094	3.70262438	0.006125	6.48304	0.0061425	6.5864247	0.006125	9.46402353	0.006165	17.4075729	0.0067475
4.17863167	0.011135	3.48292438	0.00629	5.77656294	0.0063525	7.0344347	0.00627	9.98095824	0.0063525	18.0451259	0.0068525
4.04437208	0.01126	3.79416375	0.00648	6.62088588	0.006495	7.4996724	0.006438	10.2738859	0.0064975	18.7688329	0.00706
4.49597375	0.01146833	3.90401375	0.006665	7.03443471	0.006705	7.8959912	0.006605	10.6185112	0.006725	19.5614641	0.007185
4.28848125	0.01166333	3.90401375	0.00681	6.89658294	0.00685	8.49908	0.00677	10.9803624	0.00681	20.5436429	0.007395
4.23965792	0.01178833	3.77585313	0.00698	7.68921471	0.006975	8.7920106	0.006915	11.0837471	0.0069975	21.0261088	0.0075175
5.16726708	0.01197	4.0870925	0.007145	7.32736294	0.007205	8.8609347	0.007103	11.7557641	0.0071425	21.6981218	0.007665
4.94757167	0.01213667	3.84908875	0.007355	8.20614824	0.007265	9.6363329	0.00731	12.4450071	0.0073075	22.5424482	0.0078325
4.26406958	0.01228833	3.9223175	0.0074975	7.68921824	0.007495	9.5329453	0.007415	12.8240924	0.0074775	22.6113759	0.00808
4.61802667	0.01244167	3.90401375	0.007645	8.70585294	0.0076425	9.8431065	0.007643	12.8757871	0.007685	23.5935494	0.008165
4.59361708	0.01262167	4.36171313	0.00781	8.36123059	0.0078075	10.584047	0.00781	13.0136388	0.00783	24.1621747	0.00833
5.63107375	0.012775	4.45325625	0.00804	9.49848765	0.007955	10.876978	0.007913	14.2370471	0.0079975	24.1621747	0.00852
4.95977625	0.012955	4.61902438	0.008145	9.77418529	0.008205	10.82528	0.008143	14.5472047	0.0081425	25.8163624	0.008705
5.65548542	0.01312	4.70956688	0.00831	9.44679	0.00835	11.548987	0.008228	14.9607541	0.0083525	26.1782182	0.0088525
6.1437	0.01330167	5.112345	0.008475	10.3772741	0.0086224	11.566224	0.008455	14.8918271	0.0084775	26.5056088	0.00904
5.74092167	0.01346833	4.65464188	0.008625	11.0837512	0.0086425	12.548392	0.0086	15.8050771	0.0086425	27.0742371	0.0091825
5.96061667	0.01362333	5.40527375	0.0088325	11.1699053	0.00885	12.651787	0.008833	16.2186224	0.00885	27.9357965	0.0093925
5.789745	0.01381667	5.5883525	0.0089575	10.7391294	0.0090375	12.600086	0.008915	16.5977071	0.00897	28.1598	0.0095375
6.59530167	0.013925	5.80804875	0.009165	11.3939118	0.00914	12.961945	0.009123	16.2186253	0.0091425	29.3832082	0.009685
6.021645	0.014135	4.98418813	0.00927	11.8936159	0.0092875	13.857965	0.009268	17.6143469	0.0093075	29.8139882	0.01029
5.50901875	0.0143	6.02774813	0.009435	12.18654	0.009455	13.720116	0.009393	17.9417376	0.0094775		
6.70514667	0.01448167	6.3389875	0.009645	12.4967012	0.0095175	14.564435	0.009623	18.6826759	0.0096625		
7.09571833	0.01460667	5.7531275	0.00979	12.8862471	0.00983	15.305375	0.009748	18.2002047	0.0098525		
7.18116083	0.01476	5.36865938	0.0099575	13.0480959	0.009935	15.236451	0.00985	18.8894541	0.0099975		
6.24134208	0.01496833	6.2291375	0.010165	13.2548688	0.0101625	14.926288	0.0101	19.94055	0.010185		
7.37644167	0.01509333	6.32067688	0.0103525	14.4782812	0.0103275	16.614941	0.010226	20.3885594	0.01033		
7.05910375	0.01527167	5.80805188	0.010435	14.2715076	0.0105375	16.494326	0.010475	20.1300929	0.0105175		
7.41305875	0.01545333	6.37560188	0.010605	14.7539812	0.0106625	16.649405	0.010498	21.4568924	0.0106225		
7.08351583	0.015605	6.21082688	0.0107475	14.9952147	0.01083	17.23526	0.01079	21.7870494	0.01083		
7.95009667	0.01578667	6.70514438	0.010955	15.5486094	0.0109975	17.683274	0.010935	22.0944382	0.0109975		
7.36423708	0.01598167	6.86991938	0.011165	16.1152376	0.011225	18.114046	0.010998	22.9215371	0.01108		
8.01112542	0.01609167	6.72345563	0.01129	16.8044835	0.01137	18.648214	0.011225	23.3695435	0.01133		

8.93872958	0.01625833	6.90653375	0.0114975	16.9078729	0.011515	19.45808	0.011416	23.9209412	0.0114975
7.69378458	0.01648187	7.181155	0.011865	17.4420371	0.0117025	19.871626	0.0116	24.4208424	0.0116
8.73124187	0.016605	7.291005	0.01177	17.4248041	0.01185	19.819932	0.011748	24.2827935	0.0117875
8.29184667	0.01680167	8.15148688	0.011975	17.9417371	0.0119325	20.560869	0.011915	25.7819012	0.0119775
9.52459375	0.01695333	7.80363313	0.0121025	18.0451253	0.01214	21.336274	0.012038	25.7991324	0.0121625
8.78006333	0.01709167	8.0050225	0.01231	18.6826747	0.0123075	21.749817	0.01227	26.4711459	0.0123075
8.62139167	0.01725833	7.99671188	0.012455	18.9066647	0.012615	22.301217	0.012373	26.9708459	0.012495
9.23166083	0.01743833	8.26133313	0.0126625	19.6476224	0.01262	22.869639	0.012603	27.7634841	0.01264
8.86549875	0.01760667	8.04163688	0.01283	20.0956268	0.0128475	22.300918	0.012748	27.7807118	0.0128475
9.53879333	0.01777333	8.15148375	0.012955	20.3368653	0.0129925	24.231099	0.012873	28.64227	0.012955
9.29268687	0.01798167	8.24302625	0.0131225	21.1639606	0.0131175	24.162176	0.013143	28.8145829	0.0131825
9.52459083	0.01812	8.6274975	0.01331	21.6464318	0.0133075	25.075425	0.013288	29.7967547	0.0132875
9.65885042	0.01825833	8.6091875	0.0134975	21.5775041	0.0134925	25.764672	0.013393		
9.95177917	0.01841167	9.34150913	0.0136425	22.6286088	0.01364	25.626819	0.0136		
10.5988621	0.01866187	9.54290063	0.01381	22.4735271	0.013805	26.212682	0.013703		
10.025015	0.01880167	8.883805	0.0139775	22.8181494	0.013975	26.540071	0.013933		
10.3545571	0.01898187	9.17874	0.014145	23.9209418	0.01414	27.487786	0.01408		
9.95177917	0.019105	9.32320438	0.01433	24.3344906	0.0143275	27.90133	0.014203		
10.5132263	0.0193	9.68936125	0.014475	24.6101847	0.01443	28.073842	0.014413		
10.9037996	0.01946333	9.17673626	0.0146225	25.1443529	0.01464	27.470554	0.014685		
11.282i663	0.01959167	9.89075063	0.0147475	25.1098888	0.0148275	28.435495	0.014745		
11.2211404	0.01975833	10.2386044	0.014955	26.2239124	0.0149926	28.504421	0.014915		
11.1801117	0.01993833	10.2019894	0.0151225	26.1437676	0.01512	28.84904	0.01504		
11.4774517	0.02013333	10.7512319	0.0152475	26.6951518	0.0153475	29.779521	0.01529		
11.4286329	0.02027	10.1836825	0.015475	27.5060135	0.0154725				
11.7581754	0.02045187	10.84275	0.015705	26.0920612	0.01562				
11.8192017	0.02063167	10.7695354	0.01583	26.5056129	0.015825				
12.34403	0.02075667	11.1173931	0.0159975	28.3191518	0.015995				
11.9656638	0.02093667	10.3967606	0.016145	27.4016206	0.01612				
12.3196229	0.02110333	11.3653894	0.0162675	28.1597976	0.0162285				
12.7101942	0.02129833	11.7215606	0.016475	29.5733424	0.016411				
12.4050613	0.02146687	11.9046388	0.0166625	29.5727506	0.01666				
13.22282	0.021645	11.6384781	0.016681						
13.0397396	0.02177	12.124335	0.016955						
12.7590183	0.02193833	12.5088063	0.0171425						
13.3936963	0.02209187	12.1975708	0.0173075						
13.3204629	0.0223	12.7468131	0.017455						
13.9063246	0.02243667	12.7101919	0.0176425						
13.5035467	0.02261833	12.9482025	0.017765						
14.1992533	0.0228	12.7468138	0.017995						
14.4921796	0.02290833	13.4425169	0.01812						
14.5898221	0.02309	13.22282	0.01831						
14.4189504	0.02328333	13.2594381	0.018475						
15.0414242	0.02342333	13.6822163	0.01862						
15.1834792	0.02359167	13.7903731	0.0187975						
15.1024525	0.02375833	13.7720631	0.018955						
15.2123021	0.02393833	14.1931519	0.01912						
15.7249258	0.024105	13.8819131	0.0192875						
15.6761029	0.02422833	14.3029981	0.019435						
15.9080075	0.02443833	14.3213056	0.01956						
16.0422667	0.02459	14.6874663	0.0198075						
16.1277021	0.02477	14.9987025	0.0199325						
16.3962217	0.02492333	14.57762	0.0200775						
16.774585	0.02508833	15.5479461	0.020245						
16.6525338	0.02531167	15.4930225	0.0203925						
16.9820813	0.025395	15.876105	0.02062						
17.2139808	0.025536	15.7678444	0.0207875						
17.9218942	0.02577	15.6394869	0.020975						
17.8242483	0.02592333	15.9141081	0.0211425						
17.7144013	0.02604833	16.2802688	0.02131						
17.7266108	0.02624333	16.2436544	0.021455						
17.9585108	0.02640833	16.7196856	0.0216425						
17.8364533	0.02663167	16.4450438	0.021705						
18.5077508	0.02676833	17.6716819	0.021975						
18.3612842	0.02838	16.9027475	0.02208						
18.6542154	0.02711667	17.6533744	0.022305						
18.8053936	0.02724167	17.671685	0.0224325						
19.3621313	0.02745	18.1110781	0.0225775						
19.0569956	0.02763	17.3787588	0.022785						
20.0090129	0.02774187	18.01954	0.02291						
19.8991671	0.027935	18.8434	0.02314						

Appendix B
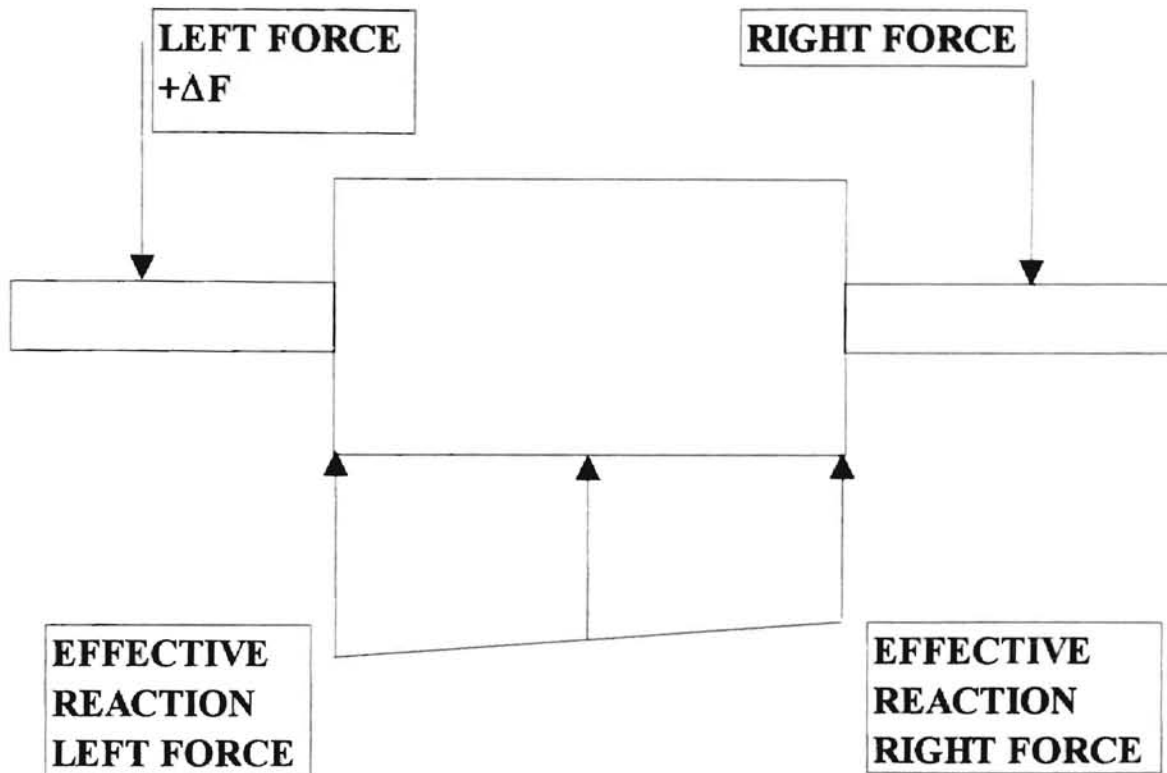
Figure B-1: Illustration of beam model developed to determine effective forces at edges of the nip

The equations developed for the reaction forces is used in the spreadsheet are given as

equations (26) and (27). Since the load applied is uneven, the load is distributed across

the width of the web. The effective forces can then be found at the edges of the web

knowing the force is linearly distributed. The equations to determine the effective force at

the edges of the web are given as equations (28) and (29).

$$QLeft = \frac{NLL}{NRW} - \frac{(NLR - NLL)*(WW)}{NRW^2} \qquad (26)$$

$$QRite = \frac{(NLR - NLL)*(WW)}{NRW^2} + \frac{NLR}{NRW} \qquad (27)$$

$$QLW = \frac{QRite - QLeft}{NRW} * 1 + QLeft \qquad (28)$$

$$QRW = \frac{QRite - QLeft}{NRW} * 7 + QLeft \qquad (29)$$

T	5.4	web tension	lbs
W	6	web width	in
h	0.002	web caliper	in
E	600000	web modulus	psi
L	71.25	web span length	in
NRD	4	nip roll diam.	in
NRW	8	nip roll width	in
NLR	74.7856131	nip load right	lbs
NLL	88.9117845	nip load left	lbs
ct	0.5	roll cover thickness	in
DURO	52	cover durometer	Shore A
WW	2.5	IN	
II	0.036	Moment of Inertia	Equation (24)
K	0.01581139	Stiffness	Equation (25)
EC	404.956603	Compression Modulus	Equation (22)
KK	0.68450848	K Factor Equation (23)	

	Y Lateral Defletion
x	Y
0	0
3.5625	0.00115666
7.125	0.00445362
10.6875	0.00963628
14.25	0.01645606
17.8125	0.02466955
21.375	0.03403777
24.9375	0.0443254
28.5	0.05530006
32.0625	0.06573153
35.625	0.07839104
39.1875	0.09005055
42.75	0.10148202
46.3125	0.11245668
49.875	0.12274431
53.4375	0.13211253
57	0.14032602
60.5625	0.1471458
64.125	0.15232846
67.6875	0.15562542
71.25	0.15678208 Max Deflection
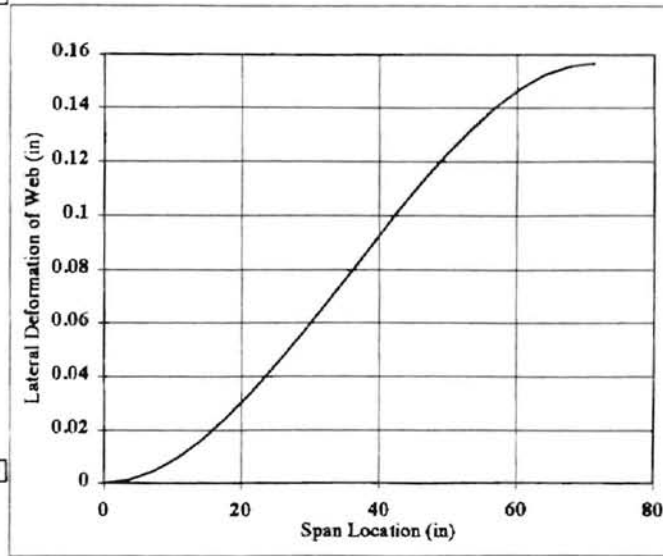
	Using Beam Model	
QRITE	8.79639807	Effective Nip Load (pli) Right Side of Nip Eq. (26)
QLEFT	11.6657766	Effective Nip Load (pli) Left Side of Nip Eq. (27)
QRW	9.15507039	Effective Nip Load (pli) Right Edge of Web Eq. (28)
QLW	11.3071043	Effective Nip Load (pli) Left Edge of Web Eq. (29)
deleps	0.00113511	Change in Strain

Solver Changed δ/t				F/W From Equation (1)		Eq. (28) and (29) From Beam Model		Eq. (20)
δ/T	ALPHA	BETA	F	F/W	δ	Qtarget	Error	ΔV/V
0.03907932	0.01406533	0.000350728	73.24056287	9.155070359	0.01954	9.155070391	3.16E-08	0.00541
0.04437254	0.01707378	0.000487554	90.45676884	11.30709611	0.02219	11.30710431	8.205E-06	0.00654
							SUMERR	
							8.236E-06	

Figure B-2: Sample calculation of lateral deflection for 52 durometer roll

T	5.4	web tension	lbs
W	6	web width	in
h	0.002	web caliper	in
E	600000	web modulus	psi
L	71.25	web span length	in
NRD	4	nip roll diam.	in
NRW	8	nip roll width	in
NLR	74.7856131	nip load right	lbs
NLL	88.9117845	nip load left	lbs
ct	0.5	roll cover thickness	in
DURO	60	cover durometer	Shore A
WW	2.5	IN	
II	0.036	Moment of Inertia	Equation (24)
K	0.01581139	Stiffness	Equation (25)
EC	615.834353	Compression Modulus Equation (22)	
KK	0.58196	K Factor Equation (23)	

	Y Lateral Deflection
x	Y
0	0
3.5625	0.00082495
7.125	0.00317641
10.6875	0.00687278
14.25	0.01173678
17.8125	0.0175948
21.375	0.02427639
24.9375	0.03161373
28.5	0.03944107
32.0625	0.04759422
35.625	0.05591
39.1875	0.06422579
42.75	0.07237893
46.3125	0.08020627
49.875	0.08754361
53.4375	0.09422521
57	0.10008323
60.5625	0.10494722
64.125	0.1086436
67.6875	0.11099505
71.25	0.11182 Max Deflection

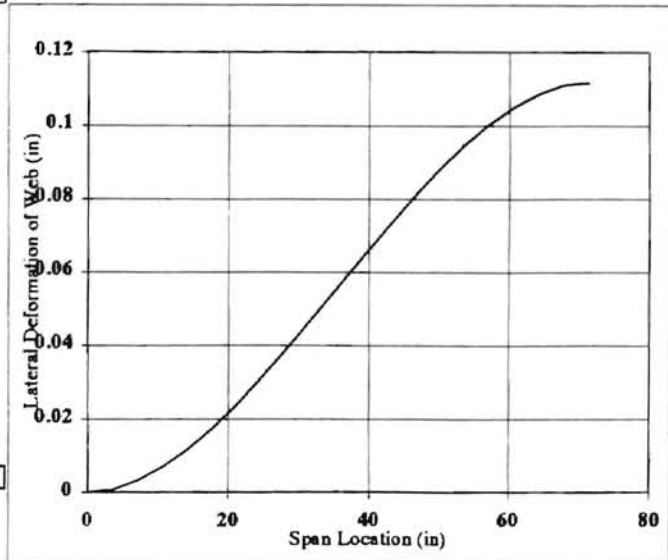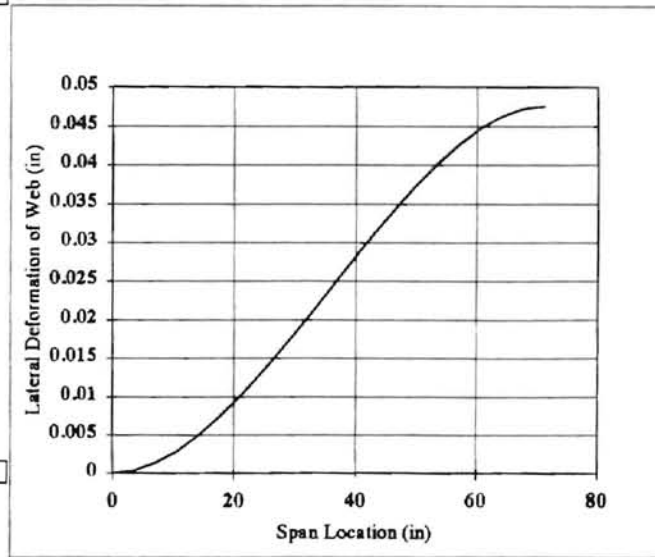|	Using Beam Model
QRITE	8.79639807	Effective Nip Load (pli) Right Side of Nip Eq. (26)
QLEFT	11.6657766	Effective Nip Load (pli) Left Side of Nip Eq. (27)
QRW	9.15507039	Effective Nip Load (pli) Right Edge of Web Eq. (28)
QLW	11.3071043	Effective Nip Load (pli) Left Edge of Web Eq. (29)
deleps	0.00080958	Change in Strain

Solver Changed δ/λ				F/W From Equation (1)		Eq. (28) and (29) From Beam Model		Eq. (20)
δ/T	ALPHA	BETA	F	F/W	δ	Qtarget	Error	$\Delta V/V$
0.03050567	0.00964939	0.000185257	73.24050513	9.155063141	0.01525	9.155070391	7.25E-06	0.00373
0.03477418	0.0117749	0.000259472	90.45683246	11.30710406	0.01739	11.30710431	2.53E-07	0.00454

	SUMERR
	7.5E-06

Figure B-3: Sample calculation of lateral deflection for 60 durometer roll

T	5.4	web tension	lbs
W	6	web width	in
h	0.002	web caliper	in
E	600000	web modulus	psi
L	71.25	web span length	in
NRD	4	nip roll diam.	in
NRW	8	nip roll width	in
NLR	74.7856131	nip load right	lbs
NLL	88.9117845	nip load left	lbs
ct	0.5	roll cover thickness	in
DURO	78	cover durometer	Shore A
WW	2.5	IN	
II	0.036	Moment of Inertia	Equation (24)
K	0.01581139	Stiffness	Equation (25)
EC	1581.57074	Compression Modulus	Equation (22)
KK	0.52504112	K Factor	Equation (23)

	Y Lateral Defletion
x	Y
0	0
3.5625	0.0003514
7.125	0.00135304
10.6875	0.00292757
14.25	0.00499946
17.8125	0.00749477
21.375	0.0103409
24.9375	0.01346636
28.5	0.01680053
32.0625	0.02027349
35.625	0.02381573
39.1875	0.02735796
42.75	0.03083092
46.3125	0.03416509
49.875	0.03729055
53.4375	0.04013668
57	0.04263199
60.5625	0.04470388
64.125	0.04627841
67.6875	0.04728005
71.25	0.04763145 Max Deflection

	Using Beam Model	
QRITE	8.79639807	Effective Nip Load (pli) Right Side of Nip Eq. (26)
QLEFT	11.6657766	Effective Nip Load (pli) Left Side of Nip Eq. (27)
QRW	9.15507039	Effective Nip Load (pli) Right Edge of Web Eq. (28)
QLW	11.3071043	Effective Nip Load (pli) Left Edge of Web Eq. (29)
deleps	0.00034486	Change in Strain

Solver Changed δ/t				F/W From Equation (1)		Eq. (28) and (29) From Beam Model		Eq. (20)
δ/T	ALPHA	BETA	F	F/W	δ	Qtarget	Error	$\Delta V/V$
0.01683321	0.00392234	4.05669E-05	73.24056308	9.155070384	0.00842	9.155070391	6.24E-09	0.0015288
0.01927791	0.00481428	5.73837E-05	90.45683462	11.30710433	0.00964	11.30710431	1.76E-08	0.0018736
							SUMERR	
							2.38E-08	

Figure B-4: Sample calculation of lateral deflection for 78 durometer roll

VITA

Noman Ahmad

Candidate for the Degree of

Master of Science

Thesis: LATERAL DEFLECTION OF A WEB DUE TO A DIFFERENTIALLY LOADED NIP

Major Field: Mechanical Engineering

Biographical:

Personal Data: Born in Calgary, Alberta, Canada, August 19, 1972, the son of Moin and Quresha Ahmad.

Education: Graduated from Union High School, Tulsa, Oklahoma, in May 1990; received Bachelor of Science Degree in Mechanical Engineering from Oklahoma State University in May 1995; completed requirements for the Master of Science Degree at Oklahoma State University in May 1997

Professional Experience: Research Assistant, Department of Mechanical and Aerospace Engineering, Oklahoma State University, June, 1995 to January, 1997; Teaching Assistant, August, 1995 to May, 1996.

Professional Memberships: Pi Tau Sigma, American Society of Mechanical Engineers.